PHYSICAL REVIEW D **91,** 096007 (2015)

High-energy vector boson scattering after the Higgs boson discovery

Wolfgang Kilian[*] and Marco Sekulla[†]
Department of Physics, University of Siegen, D-57068 Siegen, Germany

Thorsten Ohl[‡]
Faculty of Physics and Astronomy, Würzburg University, D-97074 Würzburg, Germany

Jürgen Reuter[§]
DESY Theory Group, D-22603 Hamburg, Germany
(Received 5 September 2014; published 20 May 2015)

Weak vector-boson W, Z scattering at high energy probes the Higgs sector and is most sensitive to any new physics associated with electroweak symmetry breaking. We show that in the presence of the 125 GeV Higgs boson, a conventional effective-theory analysis fails for this class of processes. We propose to extrapolate the effective-theory ansatz by an extension of the parameter-free K-matrix unitarization prescription, which we denote as direct T-matrix unitarization. We generalize this prescription to arbitrary nonperturbative models and describe the implementation as an asymptotically consistent reference model matched to the low-energy effective theory. We present exemplary numerical results for full six-fermion processes at the LHC.

DOI: 10.1103/PhysRevD.91.096007 PACS numbers: 11.55.Bq, 11.80.Et, 12.60.Cn, 12.60.Fr

I. INTRODUCTION

After the discovery of a Higgs-like particle at the LHC [1,2], and without any signal of other new particles, the focus of collider physics is shifting toward a detailed study of electroweak symmetry breaking (EWSB). We are interested in the properties of the Higgs boson itself and in its precise role in a fundamental theory [3–5]. Beyond that, the most fundamental process of the electroweak interactions is the scattering of the electroweak gauge bosons [6]. It will be one of the key physics processes at the high-luminosity LHC as well as any planned future high-energy pp and e^+e^- machine.

The most striking effect of the Higgs boson is the strong suppression of electroweak vector-boson scattering (VBS) at high center-of-mass (c.m.) energy [7]. Without the Higgs boson, VBS scattering amplitudes $VV \to VV$, where $V = W^\pm$ or Z, are dominated by scalar Goldstone-boson scattering that relates to the scattering of longitudinally polarized W and Z particles. Power counting predicts an s/v^2 rise of these amplitudes $[v = (\sqrt{2}G_F)^{-1/2} = 246\ \text{GeV}]$, such that electroweak interactions should become strong in the TeV range. However, the Standard Model (SM) representation of the Higgs sector replaces this by a consistently weakly interacting model. The cancellation induced by Higgs exchange results in a residual Goldstone-scattering amplitude that is asymptotically small, at tree level proportional to $m_H^2/v^2 = 0.25$. This can be interpreted as an effective suppression in the cross section, which for a VV c.m. energy of $\sqrt{s} = 1.2$ TeV amounts to a factor of $m_H^4/s^2 = 10^{-4}$.

At the LHC, VBS processes have become accessible to experiment [8,9]. The accuracy and energy reach of these measurements will improve at the upgraded LHC and at future colliders, including the planned ILC [10]. The SM with the observed light Higgs particle provides a very specific prediction for all VBS processes, namely a scattering amplitude that is dominated by the transversal gauge-boson components of the W and Z bosons. A significant excess in the longitudinally polarized channel would clearly point to new interactions in the EWSB sector.

A phenomenological description of high-energy VBS processes should smoothly interpolate between the low-energy behavior, which is determined by the SM and depends on a well-defined set of perturbative parameters as corrections, and any possible high-energy asymptotics, which should be captured by a sufficiently generic class of models [11,12]. It is important to note that in hadron collider observables, the separation of low- and high-energy scattering is not straightforward. For a meaningful comparison with data, the parameterized high-energy behavior has to remain consistent with the universal principles of quantum physics. Systematically comparing model predictions with data, the results will become a measure of confidence for the SM case, or otherwise the numerical evaluation of any observed new-physics effects.

In this paper, we develop this program specifically for the scenario with a light Higgs boson that is now being confirmed by the LHC analyses. This scenario deviates

[*]kilian@physik.uni-siegen.de
[†]sekulla@physik.uni-siegen.de
[‡]ohl@physik.uni-wuerzburg.de
[§]juergen.reuter@desy.de

significantly from the situation without light Higgs [13–18] where there is a steady transition from low-energy weak interactions to strong interactions at high energies. We discuss the necessary steps that allow us to parametrize high-energy asymptotics and the interpolation between low and high energies, embed this in the interacting theory with off-shell gauge bosons and fermions, and show how to convert the algorithm into a consistent calculational method and simulation of exclusive event samples.

The paper consists of three parts. In the first part, we review the essentials of the effective-theory approach to electroweak interactions and the Higgs mechanism. The second part extends the well-known concept of K-matrix unitarization in such a way that we can apply it to generic (non-Hermitian) expansions and models of the complete scattering matrix. In the third part, we show how to implement this variant of K-matrix unitarization in actual calculations of vector-boson scattering amplitudes beyond the Standard Model and show exemplary numerical results for LHC processes. In a final section, we summarize the results and conclude.

II. EFFECTIVE THEORIES FOR ELECTROWEAK INTERACTIONS

A. Effective theory and Higgs mechanism

Throughout this paper, we will assume that no new weakly coupled particles, i.e., narrow resonances, appear within the energy range that we consider for VBS. The elementary particle spectrum is given by the SM. It has been known for a long time that this scenario can be addressed by an effective field theory (EFT) as a universal phenomenological ansatz [19].

Early studies of VBS considered a nonlinear EWSB representation, the chiral electroweak Lagrangian, as an EFT without a light Higgs boson [20–31]. This scenario was to be experimentally distinguished from the simplest light-Higgs case [17,32–36]. Any Higgs-less model evolves into strong interactions in the TeV range, while the SM remains weakly interacting at all energies. However, after the recent discovery of a light Higgs candidate [1,2], new studies should narrow down the case toward distinguishing different models that do include the Higgs as a particle.

A neutral scalar particle can be coupled to the nonlinear chiral Lagrangian in a gauge-invariant way, including a power series of higher-dimensional operators [37–41]. Alternatively, we can combine it with the Goldstone bosons of EWSB as an electroweak doublet and base the analysis on the SM, also augmented by a power series of higher-dimensional operators [42–45]. Both approaches allow for the most general set of interactions. They are related by a simple field redefinition and thus equivalent [27,46–50]. However, truncating either power series exposes differences in the power counting, and thus different theoretical prejudice about the hierarchy of coefficients.

In this work, we anticipate Higgs (and W, Z) couplings that are close to their SM values, as suggested by the current LHC analyses [51]. In the linear representation, this parameter point is distinguished by renormalizablity, the absence of any higher-dimensional terms. In the nonlinear representation this parameter point is not distinguished in the Lagrangian, so the high-energy cancellations that the Higgs induces at the amplitude level appear as accidental. We therefore adopt the linear representation. Furthermore, we implicitly assume that electroweak gauge symmetry is a meaningful concept up to energies far beyond the TeV scale [46,47]. We therefore include the gauge boson fields $W_\mu^{1,2,3}$ and B_μ as elementary vector fields that enter via covariant derivatives and field strength tensors, always multiplied by the respective gauge couplings g and g' and thus weakly interacting. This assumption is clearly supported by all known electroweak precision and flavor data.

The EFT extension of the linearly parametrized SM has been worked out up to next-to-leading order in the power series (dimension six) [42,44,45,52] and applied to properties of the Higgs boson in various contexts [53–63]. Operator mixing at the one-loop order has been calculated in Refs. [64–68]. Dimension-eight operators as the second order have been studied in Refs. [69,70]. In the current work, we do not intend to incorporate the complete operator basis, but rather select exemplary terms that specifically affect VBS, such that we can describe the matching and interpolation procedure that connects low- and high-energy amplitudes.

B. Fields and operators

The SM Higgs resides in a doublet of the $SU(2)_L$ gauge symmetry. Our notation is laid out in Appendix A. We choose to parametrize the Higgs multiplet in the form of a 2×2 Hermitian matrix $\mathbf{H}$. In this parametrization, the custodial-$SU(2)_C$ transformation properties of any operator are manifest, and there is a simple relation to the nonlinear Higgs EFT, namely the replacement

$$\mathbf{H} \to \frac{1}{2}(v+h)\Sigma, \tag{1}$$

where Σ is a nonlinear Goldstone-boson representation.

Since we focus exclusively on the Higgs and electroweak gauge sectors, we do not write light fermions explicitly, but treat them as external probes for the interactions that we are interested in. In accordance with the hypothesis of minimal flavor violation, we ignore the possibility of anomalous effects due to higher-dimensional operators that involve light flavors. Heavy flavors and gluons do not play a role for the signal processes that we consider. If we do not look at observables with explicit heavy flavors, the fermion sector emerges as perturbative. Extending this result to the full EFT, we arrive at a model that decomposes, at high energy $E \gg v$, into left- and right-handed fermion, gauge

boson, and scalar (EWSB) sectors, almost mutually decoupled due to the smallness of the EWSB order parameter v. This decomposition is stable against radiative corrections, since operator mixing in the EFT is governed exclusively by weak couplings with loop factors. It should be noted that it is also stable with respect to applying equations of motion to the operator basis, as long as we impose the gauge and minimal flavor violation principles that identify weak coupling parts.

The processes of interest at a hadron collider, namely

$$pp \to 2j + (VV \to 4f), \tag{2}$$

embed the actual quasielastic VBS processes, $VV \to VV$, together with an irreducible non-VBS background. The vector-boson interactions are affected by all bosonic dimension-six and dimension-eight operators that the EFT provides. We should weigh their impact in view of the experimental possibilities. Current and future analyses will rather precisely determine the coefficients of pure-gauge operators that affect vector-boson pair production and related processes. Fixing a suitable operator basis, we may take these coefficients as given [71,72]. On the other hand, we can safely ignore terms that exclusively provide couplings to Higgs pairs, since such couplings do not enter VBS processes at tree level. In a simplified first approach to the problem, we may thus exclude most dimension-six operators from an analysis that focuses on VBS. Instead, we incorporate operators that supply genuine quartic gauge couplings in the longitudinal mode. Such operators do not affect simpler processes; they occur first at dimension eight in the operator basis.

For the purpose of studying VBS processes, we therefore concentrate on the subset

$$\mathcal{L}_{HD} = F_{HD}\mathrm{tr}\left[\mathbf{H}^\dagger\mathbf{H} - \frac{v^2}{4}\right] \cdot \mathrm{tr}[(\mathbf{D}_\mu\mathbf{H})^\dagger(\mathbf{D}^\mu\mathbf{H})], \tag{3}$$

$$\mathcal{L}_{S,0} = F_{S,0}\mathrm{tr}[(\mathbf{D}_\mu\mathbf{H})^\dagger\mathbf{D}_\nu\mathbf{H}] \cdot \mathrm{tr}[(\mathbf{D}^\mu\mathbf{H})^\dagger\mathbf{D}^\nu\mathbf{H}], \tag{4}$$

$$\mathcal{L}_{S,1} = F_{S,1}\mathrm{tr}[(\mathbf{D}_\mu\mathbf{H})^\dagger\mathbf{D}^\mu\mathbf{H}] \cdot \mathrm{tr}[(\mathbf{D}_\nu\mathbf{H})^\dagger\mathbf{D}^\nu\mathbf{H}]. \tag{5}$$

The corresponding Feynman rules modify the VBS amplitude expressions, predominantly in the longitudinally polarized channel.

The dimension-six operator $\mathcal{L}_{HD}$ modifies the HWW and HZZ couplings and thus controls the Higgs exchange diagrams in VBS. We take this particular term as a representative of the possible effects that dimension-six operators can contribute to VBS processes. We have written the operator in a subtracted form, such that it respects on-shell renormalization conditions as discussed in Appendix A.

The included terms manifestly respect custodial symmetry, $SU(2)_C$ [73]. There are both dimension-six and dimension-eight operators that violate $SU(2)_C$, but they provide bilinear and trilinear gauge couplings and thus should be considered as input to a VBS analysis. $SU(2)_C$-violating operators that only affect quartic couplings occur first at dimension 10. This is a consequence of the linear doublet Higgs representation. We therefore assume global $SU(2)_C$ invariance for the current paper, which should hold at least at the threshold where new effects start to become relevant.

C. Breakdown of the EFT

The pure-SM cross section for VBS, (2), is dominated by transversally polarized gauge bosons, which in the high-energy limit decouple from the Higgs sector. Apart from the Higgs suppression, this is a consequence of the vector-boson production mechanism, namely radiation from massless fermions that couple to longitudinal vector bosons only via helicity mixing [74,75]. The transversal polarization directions are further enhanced by their higher multiplicity.

Adding in the operators (3)–(5), the picture changes. In Fig. 1, we illustrate this for the particular process of same-sign W production at a LHC energy of 14 TeV. We have applied standard cuts [8] on the forward jets and the VV system, adapted to the simplified picture of on-shell vector bosons in the final state.

For this figure, we have computed the complete process $pp \to W^+W^+jj$ at leading order. We used the Monte Carlo integrator and event generator WHIZARD [76–78] with the CTEQ6L PDF set. The SM curve is compared to three curves for models that contain a single nonzero coefficient for the

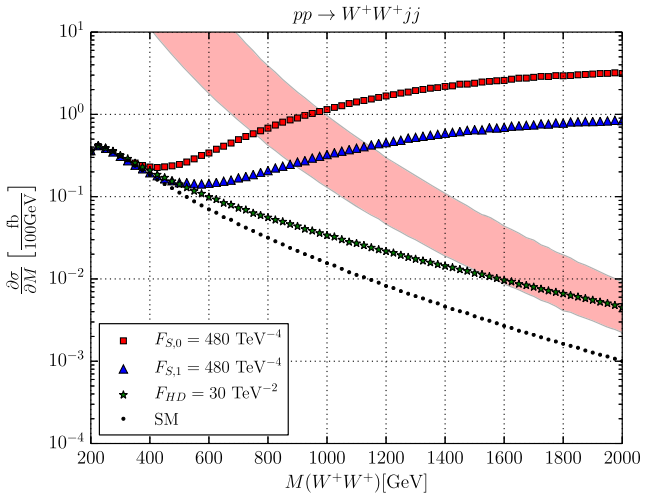

FIG. 1 (color online). $pp \to W^+W^+jj$, naive EFT results that violate unitarity, QCD contributions neglected. The band describes maximal allowed values, due to unitarity constraints, for the differential cross section. The lower bound describes the saturation of $\mathcal{A}_{20}$, and the upper bound describes the simultaneous saturation of $\mathcal{A}_{20}$ and $\mathcal{A}_{22}$; cf. (47). Cuts: $M_{jj} > 500$ GeV; $\Delta\eta_{jj} > 2.4$; $p_T^j > 20$ GeV; $|\eta_j| > 4.5$.

effective higher-dimensional operators [Eqs. (3), (4), (5)], respectively, without any unitarization correction. For an indication of the unitarity limits, we have included a quartic Goldstone interaction amplitude with a constant coefficient $a_{IJ} = \mathrm{i}$ in the $I = 2$ and $J = 0, 2$ channels and recomputed the process with this modification. The variation in the unitarity bound corresponds to the choice of saturating only one or both of these contributions. This amplitude has been extended to physical vector bosons at finite energy and evaluated for off-shell initial-state vector bosons, according to the prescription that we describe below in Sec. IV C. Because of the inherent ambiguities in such a prescription for finite energy, it is not possible to precisely state the unitarity limits for a physical cross section. Nevertheless, we should constrain the validity region of the effective theory, given the chosen parameter values, to the energy range where the unitarity band is not yet touched by the corresponding curve.

The cross section with a dimension-six correction included, asymptotically falls off with a slower rate than the SM reference curve. There is a range of coefficient values for which the EFT remains valid, until it eventually crosses the unitarity bound. Looking at Fig. 1, we observe that for the chosen coefficient value, unitarity can be regarded as (marginally) satisfied, if we account for the limited event count in an actual analysis that makes the lower part of the diagram inaccessible. For larger coefficient values, we would leave the applicability range of the EFT. This result is typical for the effect of dimension-six operators in energy-dependent observables [63,79].

By contrast, the dimension-eight operators have a dramatic impact on the VV pair invariant-mass distribution. The differential cross section leaves the SM value at a certain threshold energy and then *increases* up to a broad maximum at multi-TeV invariant mass. This behavior is easily explained by the high mass dimension of the included operators. Their contributions are enhanced by M_{WW}^8/m_H^8 relative to the SM prediction. The high power of M_{WW} overcomes the energy-dependent suppression caused by the parton distributions. Taken at face value, this would become a powerful handle on the coefficients $F_{S,0}$ and $F_{S,1}$, even for a rather low collider luminosity.

Unfortunately, this result is entirely unphysical. No high-energy completion of the SM that is consistent with the basic assumptions of the EFT approach is capable of producing such a distribution [7]. In the dimension-eight case, the calculated curves cross this unitarity limit immediately within the experimentally accessible region, for *any* coefficient value that could possibly be accessible. Furthermore, except for the rare final state $ZZ \to 4\ell$, observables at a hadron collider mix different M_{WW} ranges and thus disallow a strict exclusion of the unphysical region in an analysis.

Obviously, we are using the EFT far beyond its region of validity. The important result is that for the dimension-eight operators, which are the most interesting terms in this context, there is actually *no* coefficient value for which the EFT yields a useful prediction. This is in contrast to an analysis of dimension-six operators, which are mostly accessible via production and decay processes with well-defined or limited energy range. In other words, if a deviation from the SM in VBS can be detected at all, it either contains new particles that invalidate the SM-based EFT or it contains strong interactions. In either case, the pure EFT is insufficient.

III. UNITARIZATION PRESCRIPTIONS

A. K-matrix ansatz, Cayley transform and stereographic projection

To address the invalid high-energy asymptotics of an EFT in a universal way, we start with the K-matrix ansatz. The formalism applies to the complete S matrix, so it is independent of any particular model or approximation, and it does not rely on a perturbative expansion. It is therefore a suitable ansatz for the present problem where we have no clue about the fundamental theory that describes electroweak interactions, unless it is just the Standard Model or a simple weakly interacting extension.

Heitler [80] and Schwinger [81] introduced the K operator as the Cayley transform of the complete unitary scattering operator S, namely

$$S = \frac{\mathbf{1} + \mathrm{i}K/2}{\mathbf{1} - \mathrm{i}K/2}, \tag{6a}$$

where we include a factor of $1/2$ for later convenience. K is self-adjoint by definition, and as such more closely related to the interaction Hamiltonian than the S matrix. The corresponding transition operator T, as defined by $S = \mathbf{1} + \mathrm{i}T$, is then

$$T = \frac{K}{\mathbf{1} - \mathrm{i}K/2}. \tag{6b}$$

This T satisfies the optical theorem $\mathrm{i}T^\dagger T = T - T^\dagger$ since S is unitary, $SS^\dagger = S^\dagger S = \mathbf{1}$.

These relations can be inverted

$$K = 2\mathrm{i}\frac{1 - S}{1 + S} = \frac{T}{1 + \mathrm{i}T/2}. \tag{7}$$

If the theory admits a perturbative expansion, the latter formula allows us to compute the K-matrix perturbatively from the expansion of T, as long as $T - 2\mathrm{i}$ is nonsingular. Obviously, $K = T$ in lowest order.

If we are able to find a basis that diagonalizes the scattering operator S, and thus T and K, the Cayley transform has a simple geometric interpretation for the eigenvalues. Given a complex eigenvalue $t = 2a$ of the true transition operator T, the optical theorem implies

$$|a - \mathrm{i}/2| = 1/2; \tag{8}$$

i.e., the eigenamplitude a is located on the Argand circle with radius $1/2$ and center $\mathrm{i}/2$ [82]. The corresponding real K-matrix eigenvalue $k = 2a_K$ is then given by

$$a_K = \frac{a}{1 + ia}. \tag{9}$$

This is the inverse of the stereographic projection from the real axis onto the Argand circle; cf. Fig. 2. The Cayley transform, or K matrix, can thus be understood as the inverse stereographic projection of the transition matrix T onto the space of Hermitian matrices.

The scattering amplitude of charged particles will contain a Coulomb singularity. This singularity is physical and must not be handled by an *ad hoc* unitarization prescription, but by a proper definition of the asymptotic states of charged particles [83–86] instead. Thus one should subtract the Coulomb singularity from the amplitude, apply the chosen unitarization prescription to the remainder, and subsequently add the Coulomb singularity together with appropriate corrections for the asymptotic states.

In the following, we will use the terms scattering operators and scattering matrices interchangeably. We stress that we are always dealing with the full $2 \to n$-particle scattering operators. Nevertheless, we may assume that we work in the finite dimensional subspaces corresponding to a fixed overall angular momentum in the partial wave decomposition.

B. Standard K-matrix unitarization

Following Gupta and collaborators, and subsequent studies [32,87–90], we may reverse the logic behind the definition of the K matrix. We interpret the Hermitian K matrix as an incompletely calculated approximation to the true amplitude and look for the unitary S or T matrix as a nonperturbative completion of this approximation.

Let us first assume that the scattering matrix is available in diagonal form. Given a real eigenamplitude a_K (9) of the K matrix, the corresponding unitarized amplitude a that enters the T matrix is obtained by inverting (9),

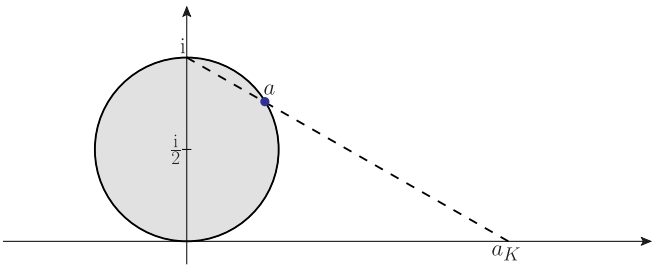

FIG. 2 (color online). Stereographic projection of a real scattering amplitude (K-matrix eigenvalue) onto the Argand circle.

$$a = \frac{a_K}{1 - \mathrm{i}a_K}. \tag{10}$$

If the approximation to the scattering matrix K is Hermitian but not available in diagonal form, we can similarly define the unitarized transition matrix T as the stereographic projection, by the formula (6b).

The standard K-matrix unitarization formalism works on a perturbative series of the T matrix. Given an nth order approximation $T_0^{(n)}$ to the T matrix, represented by an eigenamplitude $a_0^{(n)}$, we first have to construct the corresponding real K-matrix amplitude $a_K^{(n)}$ via (9),

$$\begin{aligned} a_K^{(n)} &= \frac{a_0^{(n)}}{1 + \mathrm{i}a_0^{(n)}} \\ &= a_0^{(1)} + \mathrm{Re}a_0^{(2)} + \mathrm{i}(\mathrm{Im}a_0^{(2)} - (a_0^{(1)})^2) + \cdots \\ &= a_0^{(1)} + \mathrm{Re}a_0^{(2)} + \cdots, \end{aligned} \tag{11}$$

where we assume that $a_0^{(1)}$ is real and use the lowest order of the optical theorem $\mathrm{Im}a_0^{(2)} = (a_0^{(1)})^2$. At each order, the imaginary parts cancel if the original perturbation series was correct. In a second step, we then insert the truncated perturbation series for $a_K^{(n)}$ into (10), this time without truncating,

$$a^{(n)} = \frac{a_0^{(1)} + \mathrm{Re}a_0^{(2)} + \cdots}{1 - \mathrm{i}(a_0^{(1)} + \mathrm{Re}a_0^{(2)} + \cdots)}. \tag{12}$$

If the exact scattering matrix does admit a perturbative expansion, this prescription amounts to a partial resummation of the perturbation series. In its general form, the construction guarantees that (i) the computed S matrix is unitary, and (ii) perturbation theory is reproduced order by order.

For a concrete example, a $2 \to 2$ scattering process of scalar particles with a scalar s-channel pole is represented by a $J = 0$ partial-wave eigenamplitude

$$a_K^{(0)}(s) = \frac{\lambda}{s - m^2}, \tag{13}$$

and the unitarized version reads

$$a^{(0)}(s) = \frac{\lambda}{s - m^2 - \mathrm{i}\lambda}, \tag{14}$$

the Breit-Wigner form of a scalar resonance. K-matrix unitarization, in this case, therefore implements the Dyson resummation of the resonant propagator.

Beyond leading order, given the (nonunitary) perturbative approximation to the transition matrix T, we should reconstruct the corresponding truncated perturbative

expansion of the Hermitian K matrix via (7) and insert this back into the unitarization formula (6b), to obtain the corresponding unitarized T matrix. Thus inserting an nth order approximation of (7) into (6) will result in a unitary S matrix to *all* orders. Conversely, the nth order expansion of this S matrix will reproduce the original nth order expression, which is unitary only up to terms of order $n+1$.

C. Direct T-matrix unitarization I: Linear projection

While the reconstruction of the unitary S (or T) matrix according to this algorithm is exact within the framework of perturbation theory, it suffers from the drawback that we have to reconstruct the self-adjoint K matrix as an intermediate step. This is not just unnecessary, but it may become a significant complication if the scattering matrix is not available in diagonal form, or if nonperturbative effects need to be considered. For practical purposes, we are rather interested in a means to unitarize an arbitrary *model* of the scattering matrix, which may or may not admit a perturbative expansion.

In the following, we therefore present a generalization of the K-matrix prescription that operates on the T matrix directly. Given a_0 as a *complex* approximation to an eigenvalue of the true T matrix, we first define the unitarized version a by the same geometric construction as before, i.e., connecting the point a_0 with the point i by a straight line and determining the intersection with the Argand circle. However, we do not attempt to construct the real amplitude a_K. This results in

$$a = \frac{\mathrm{Re}a_0}{1 - \mathrm{i}a_0^*}. \tag{15}$$

This formula has the properties that (i) a lies on the Argand circle, (ii) if a_0 is real, it reproduces (10), and (iii) if a_0 is already on the Argand circle, it is left invariant, $a = a_0$. This guarantees the invariance of the correct perturbative series, up to the resummation of higher orders. Nevertheless, the actual expression for (15), evaluated in perturbation theory, differs from the standard K-matrix formula (12). We obtain

$$a^{(n)} = \frac{a_0^{(1)} + \mathrm{Re}a_0^{(2)} + \cdots}{1 - \mathrm{i}(a_0^{(1)} + \mathrm{Re}a_0^{(2)} - \mathrm{iIm}a_0^{(2)} + \cdots)}. \tag{16}$$

Because of the truncation of the perturbation series at different stages of the calculation, higher orders enter in a different way. We also note that the standard K-matrix formalism, and thus formula (16), *requires* the existence of a perturbative series. By contrast, the direct unitarization formula (15) does not rely on a perturbative expansion. The latter construction is thus applicable to a larger set of models. In particular, in the case of vector-boson scattering with a light Higgs that we consider in this paper, the leading term $a_0^{(1)}$ is suppressed, and thus the original K-matrix construction is ill behaved. The modified version (15) does not suffer from this problem.

Still, the formula (15) is not quite satisfactory: if the imaginary part of a_0 becomes larger than i, the selected intersection point a appears beyond the fixed point $a = \mathrm{i}$, on the complex half-plane opposite to the location of a_0. A consequence would be that a model amplitude of the form

$$a_0(s) = \frac{\lambda'}{s - m^2 - i\lambda}, \tag{17}$$

where $\lambda' > \lambda$, would be transformed into a unitarized version that revolves *twice* around the Argand circle, splitting the resonance at m^2 into two separate peaks. Although the original model is a rather pathological ansatz for a resonance, such a behavior is clearly undesirable. To avoid this problem, we may require that (iv) if $\mathrm{Im}a_0 \geq 1$, the unitarized amplitude a is tied to the fixed point, i.e., we finally define

$$a = \begin{cases} \frac{\mathrm{Re}a_0}{1 - \mathrm{i}a_0^*} & \text{if } \mathrm{Im}a_0 < \mathrm{i}, \\ \mathrm{i} & \text{otherwise.} \end{cases} \tag{18}$$

We now generalize this prescription to the scattering matrix T, starting from a model approximation T_0 that is not necessarily unitary. We may first restrict ourselves to matrices that are normal (i.e., $T_0^\dagger T_0 = T_0 T_0^\dagger$) and do not have eigenvalues with an imaginary part larger than i. The unitarized transition matrix then is given by

$$T = \frac{\mathrm{Re}T_0}{\mathbf{1} - \frac{\mathrm{i}}{2}T_0^\dagger}. \tag{19}$$

For non-normal matrices, the operator ordering in the fraction must be defined. We obtain two equivalent expressions

$$\begin{aligned} T &= \frac{1}{\sqrt{\mathbf{1} - \frac{1}{2}\mathrm{Im}T_0}}\mathrm{Re}T_0\frac{1}{\mathbf{1} - \frac{\mathrm{i}}{2}T_0^\dagger}\sqrt{\mathbf{1} - \frac{1}{2}\mathrm{Im}T_0} \\ &= \sqrt{\mathbf{1} - \frac{1}{2}\mathrm{Im}T_0}\frac{1}{\mathbf{1} - \frac{\mathrm{i}}{2}T_0^\dagger}\mathrm{Re}T_0\frac{1}{\sqrt{\mathbf{1} - \frac{1}{2}\mathrm{Im}T_0}}. \end{aligned} \tag{20}$$

For any matrix T_0, the matrix T from (20) respects the optical theorem. If T_0 already respects the optical theorem, we get $T = T_0$. If T_0 represents the correct perturbative expansion of T, truncated at a given order and retaining non-Hermitian parts, the reconstructed matrix T reproduces this perturbative expansion.

Beyond perturbation theory, in order to extract eigenvalues with imaginary parts greater than i, either we may diagonalize the matrix and use (18) or we can use

projections to make (20) well defined. For this purpose, recall that functions of matrices can be defined by their power series expansion, as long as the radius of convergence exceeds the norm of the matrix. More generally, one can use a functional calculus to associate with a function $f: D \subseteq \mathbf{C} \to \mathbf{C}$ a function $\hat{f}$ mapping matrices to matrices, such that

$$\widehat{\alpha f + \beta g} = \alpha \hat{f} + \beta \hat{g}, \tag{21a}$$

$$\widehat{fg} = \hat{f}\,\hat{g}, \tag{21b}$$

$$\widehat{f \circ g} = \hat{f} \circ \hat{g}. \tag{21c}$$

The Riesz-Dunford functional calculus [91–93] defines $\hat{f}(A)$ by a contour integral encircling the spectrum $\sigma(A)$

$$\hat{f}(A) = \int_{\partial\Sigma:\sigma(A)\subseteq\Sigma} \frac{\mathrm{d}z}{2\pi \mathrm{i}} \frac{f(z)}{z\mathbf{1} - A} \tag{22}$$

using the fact that the resolvent matrix $1/(z\mathbf{1} - A)$ is well defined whenever $z \notin \sigma(A)$. Note that this functional calculus can be used unchanged for all bounded operators on a Hilbert space. It can even be extended to certain classes of unbounded operators, but the details are not important in the present work, because we deal with finite dimensional matrices corresponding to scattering amplitudes with definite angular momentum. Closely related to this functional calculus (22) are the projections on the invariant subspace of A corresponding to a part $\Sigma \subseteq \sigma(A)$ of the spectrum [91–93]

$$P_{A,\Sigma} = \int_{\partial\Sigma} \frac{\mathrm{d}z}{2\pi \mathrm{i}} \frac{1}{z\mathbf{1} - A}. \tag{23}$$

In particular, we can define projections $P_{\mathrm{Im}T_0/2,\Sigma_\pm}$ with

$$\mathbf{1} = P_{\mathrm{Im}T_0/2,\Sigma_+} + P_{\mathrm{Im}T_0/2,\Sigma_-} \tag{24}$$

using the contours $\Sigma_\pm$ in Fig. 3 to generalize the prescription (18) for $\mathrm{Im}T > 2$.

D. Direct T-matrix unitarization II: Thales projection

Elementary geometry (Thales' theorem) suggests an alternative construction of the stereographic projection from the real axis to the unitarity circle, which results in a different extension to general complex scattering amplitudes. Figure 4 shows that the K matrix amplitude a_0 coincides with the end point of a half-circle that connects the lower fixed point 0 with the unitary amplitude a. Consequently, given an arbitrary complex amplitude a, we define the Thales projection a as the intersection point of the half-circle that connects 0 and a_0, with the Argand

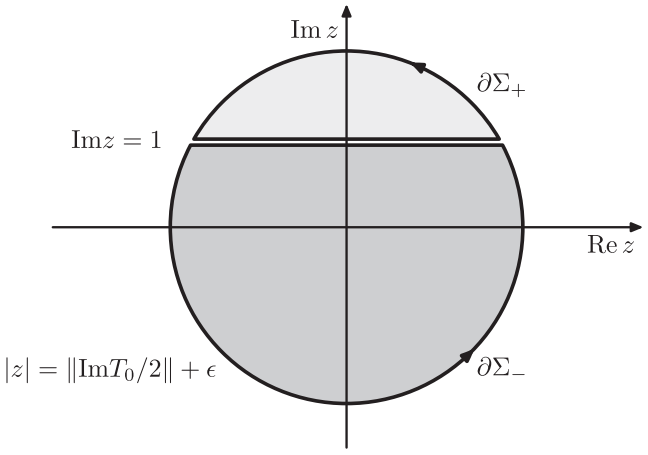

FIG. 3. Integration contours used for projecting on the subspaces corresponding to $\mathrm{Im}T_0/2 < 1$ and $\mathrm{Im}T_0/2 > 1$ for a bounded operator $\mathrm{Im}T_0/2$ in (20).

circle. The Thales circle is characterized by its intersection a_K with the real axis, given by

$$\left| a - \frac{a_K}{2} \right| = \frac{a_K}{2}. \tag{25}$$

Therefore every real amplitude a_K would be projected on the unitary circle

$$a = \frac{a_K}{1 - \mathrm{i}a_K}. \tag{26}$$

In case we start with a complex amplitude a_0, we can derive the transformation to real a_K from the condition that a_0 has to be on the Thales circle, (25), see Fig. 5,

$$\frac{1}{a_K} = \frac{\mathrm{Re}(a_0)}{|a_0|^2} = \mathrm{Re}\left(\frac{1}{a_0}\right). \tag{27}$$

We then calculate the transformation for general amplitudes,

$$a = \frac{1}{\mathrm{Re}(\frac{1}{a_0}) - \mathrm{i}}. \tag{28}$$

The corresponding operator equation is

$$T(T_0) = \frac{1}{\mathrm{Re}(\frac{1}{T_0}) - \frac{\mathrm{i}}{2}\mathbb{1}}. \tag{29}$$

In Appendix B we show that this indeed leads to a unitary S operator, and that the T operation on a T_0 operator is idempotent.

This construction avoids the undesirable behavior for a model amplitude above the Argand circle; the unitarized version of a single resonance is again a single resonance. However, it suffers itself from another undesirable feature:

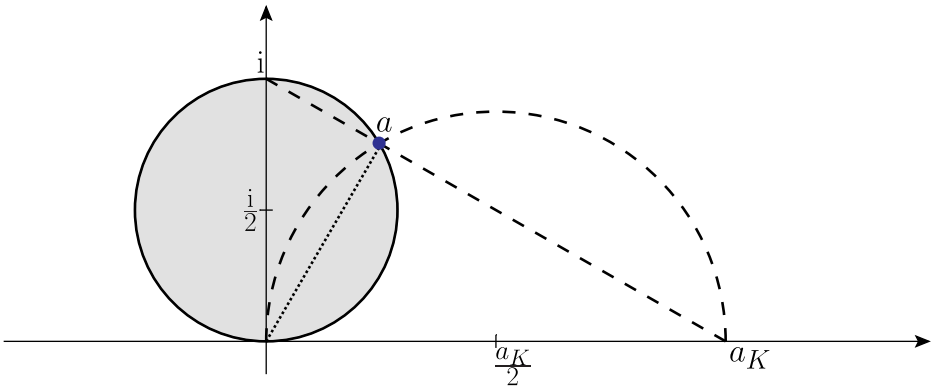

FIG. 4 (color online). Geometrical representation of Thales projection.

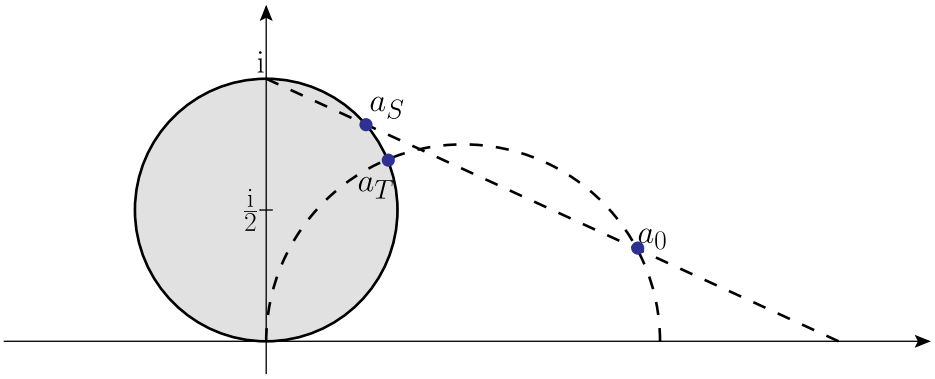

FIG. 5 (color online). Geometrical representation: stereographic projection vs Thales projection.

it is not analytic in the vicinity of $a_0 = 0$. Fortunately, this drawback is of little practical importance, because we are mostly interested in the case where $a_0 \neq 0$.

E. Alternative unitarization prescriptions

The direct T-matrix projection, as described above, allows us to unitarize any model of the scattering matrix without relying on perturbation theory or any other details of the processes under consideration. It leaves invariant the scattering matrix, if it is already unitary. Nevertheless, it is clearly not unique. Since the model that we start from does not carry the complete information about its UV completion, we cannot expect the correct completion to appear in the unitarized version either.

For an instructive example, consider another parameterless prescription,

$$S = e^{iL}, \tag{30a}$$

$$T = 2e^{iL/2}\sin\frac{L}{2}, \tag{30b}$$

which leads to

$$L = -i\ln S = -i\ln(1 + iT). \tag{31}$$

In a perturbative expansion[1] away from the cut starting at $T = -i\mathbf{1}$, the logarithm will be replaced by a polynomial and L will grow like a power, as the coupling and energy increase. In this case, unlike (6), the S matrix will "wrap around" faster and faster, corresponding to a series of resonances with decreasing distance.

We do not expect a unitarization prescription to produce additional structure that is not already present in the original model. However, the tower of resonances that appear in (30) clearly is an artifact of the prescription. From this perspective, the prescription (6), which for a uniformly growing amplitude just implies asymptotic saturation and

[1]Incidentally, the expansions of L and K agree in first and second orders:

$$K = T - \frac{i}{2}T^2 - \frac{1}{4}T^3 + \cdots, \tag{32a}$$

$$L = T - \frac{i}{2}T^2 - \frac{1}{3}T^3 + \cdots. \tag{32b}$$

no extra features, appears to be closer to a minimal and thus natural amendment of the perturbative prediction.

There are also unitarization prescriptions that rely on reordering a perturbation series, such as Padé unitarization [94–96], which has frequently been applied to vector-boson scattering physics in the Higgs-less or heavy-Higgs limit [32,97–100]. This method reproduces certain exactly solvable models [101]. Unitarization prescriptions of this kind tend to generate resonances (poles) at higher energy that are not present in the original EFT. Similar effects are observed when applying the inverse-amplitude [102–106] or N/D unitarization prescriptions [103,107]. This may be useful if the amplitude in the correct UV completion actually contains those resonances (as in pion-pion scattering).

Other approaches explicitly apply a form-factor suppression to amplitudes that nominally violate unitarity constraints [108–111]. Such a suppression indicates new physics, e.g., mixing with nearby resonances or additional open channels that dissipate the scattering into multiparticle final states. This is a possible scenario for high-energy electroweak interactions, but it is not a prediction of unitarity [79]. The form factors depend on additional parameters. To implement such a behavior, one would describe the new physics explicitly.

F. Unitarization as a framework

In the example computations below, we explicitly apply direct T-matrix projection to quasielastic scattering in the Goldstone limit, at tree level, and extend the results to full scattering amplitudes and cross sections. At this level, it coincides with the K-matrix prescription for elastic scattering, analogously extended. However, we emphasize that the direct T-matrix method is of a generic nature, since it allows us to unitarize any model for any class of processes, limited just by calculability of the actual expressions.

In particular, we may consider loop-corrected EFT amplitudes as the starting point for unitarization. These amplitudes provide an imaginary part, which is correctly treated by the prescription and accounted for in the resummation. The resummation corrects the perturbative amplitude by terms that are formally of higher order, but become relevant and restore unitarity once the growing amplitude enters the strongly interacting regime. Likewise, we may choose to insert an amplitude that has already been unitarized by any of the above mentioned unitarization prescriptions. In that case, the T-matrix prescription will leave the amplitude unchanged. Furthermore, it is possible to apply the method to all polarization components of vector bosons, without recourse to the Goldstone limit, and to properly incorporate $2 \to n$ processes.

In short, the prescription that we propose serves as a *framework* that we can implement not just for the extrapolation of the tree-level EFT result (see below) but to any more sophisticated description of VBS or electroweak processes in general.

In the following section, we evaluate the direct T-matrix projection for the minimal EFT with anomalous couplings, as a simple application. We do not expect a UV complete model to emerge. The implemented asymptotics is minimal, interpolating the low-energy EFT with high-energy unitarity saturation for any parameter set different from the SM. We propose to take this as a class of reference models. As soon as experiment will allow us to inspect the high-energy behavior in more detail, we should introduce specific extensions, such as new resonances or other kinds of new physics, similarly applying T-matrix projection where necessary. Such refined models, which could be the result of one of the more predictive schemes as discussed above, can then be compared to the reference model in the analysis of actual data.

IV. UNITARY DESCRIPTION OF ELECTROWEAK INTERACTIONS

A. Unitarity for electroweak scattering amplitudes

In the current paper, we are interested in a model-independent bottom-up approach to VBS processes. The Higgs-induced cross-section suppression makes VBS a prime candidate for looking at anomalous effects. Furthermore, there are possible extensions of the SM that provide large (tree-level) contributions exclusively to the quartic couplings, via resonance exchange in s and t channels, but only minor contributions to dimension-six operators in the EFT [112].

Results from analyzing VBS data should be combined with all kinds of different measurements, many of which remain well defined in the EFT. However, the EFT breakdown within the accessible region inevitably introduces a model dependence. We should set up the phenomenological description in such a way that this model dependence is kept under control.

The fundamental process in question is a quasielastic $2 \to 2$ scattering process of Goldstone bosons. The unitarity requirement takes a particularly simple form, since we can employ angular-momentum and isospin symmetry to completely diagonalize the scattering process. The eigenamplitudes are just scalar functions of s that must satisfy the Argand-circle condition (8) as long as no inelastic channels appear.

In reality, we should face one of the following situations:

(1) The amplitude stays in the perturbative regime, close to zero, and the imaginary part is small compared to the real part. This is the SM case.
(2) The amplitude rises beyond this level. Then, it will develop an imaginary part, and we are in a strongly interacting regime. This happens if there is any dimension-eight operator with a noticeable coefficient.
(3) The amplitude approaches the maximum absolute value, asymptotically (Fig. 6, left).

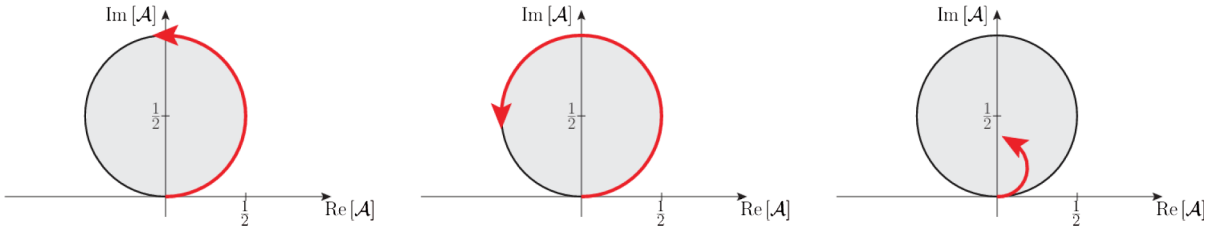

FIG. 6 (color online). The Argand-circle condition for a scattering amplitude.

(4) The amplitude turns over. This is a resonance (Fig. 6, center).
(5) New inelastic channels open and absorb part of the total cross section (Fig. 6, right). This amounts to an increase in the amplitude that is halted by an effective form-factor suppression. The extra channels, typically resulting in multiple vector boson production, should then be observable [13,113].

For a prediction, we have to make a choice among these possibilities. There is no case where the amplitude (in the ideal case of pure Goldstone scattering) leaves the Argand circle, so the naive EFT result is no option.

In general, apart from the exact SM case we are necessarily in a nonperturbative regime. In line with the discussion in the preceding section, we propose to take case 3 as a reference model for the high-energy behavior, correctly matched to the low-energy EFT. This idea is realized by the parameter-free direct T-matrix unitarization prescription, as an extension of the K-matrix unitarization formalism as described in the preceding section. In the high-energy range, the results saturate the unitarity bound. We thus obtain an approximate *upper bound* for the set of possible amplitudes that match a given EFT.

We recall that the T-matrix prescription is not a viable UV completion of the EFT but should be understood as a safeguard against computing unphysical contributions beyond the unitarity limit. In the case at hand, the unitarization changes the interpretation of EFT operator coefficients. While they formally remain the parameters of a low-energy Taylor expansion of the cross section, they effectively take the role of threshold parameters that indicate the point of energy where the differential cross section deviates from the SM prediction and enters a strongly interacting regime. This threshold region is the energy range to which the experimental analysis will be most sensitive. In a context where the EFT applies, they keep their relation to the full set of operator coefficients that may be determined by a global fit to experimental results. The high-energy range where actual model dependence becomes important is asymptotically suppressed in the same way as the SM prediction and has a minor impact on observed experimental data, as one would expect.

A complete description of the processes in question should aim at a more detailed understanding. Such a refinement typically relies on more specific assumptions or introduces new parameters. However, the first measurements of VBS will not be very sensitive to details beyond threshold, so simulations based on a simple unitarization prescription in the EFT context will at least allow us to quantify the level of agreement (or disagreement) of data with the SM.

B. Model and calculation: Amplitudes

There are various refinements that we must apply to the idealized model of the preceding section. (i) We have to translate Goldstone-boson interactions to interactions of vector bosons. This introduces the explicit $SU(2)_C$ breaking associated with hypercharge. (ii) Further low-energy corrections are caused by the mixing of transversal and longitudinal (effectively scalar) polarization components. This mixes spin and orbital angular momentum and spoils the simplicity of the partial-wave expansion. (iii) The vector bosons are off shell, in particular in the initial state. (iv) In the forward scattering direction, massless photon exchange becomes relevant, cut off only by the off-shellness of the vector bosons in the initial state, and thus a significant correction.

We approach this situation by the following algorithm. First, we analytically unitarize the scattering amplitudes in the high-energy limit where the symmetries are exact, and the unitarity-violating terms occur exclusively in Goldstone-boson scattering. In particular, we can make use of custodial, i.e., weak isospin symmetry and thereby reduce the number of independent amplitudes.

In contrast to the no-Higgs case that has been discussed extensively in the literature, in the presence of a light Higgs boson, the SM contribution to Goldstone scattering is asymptotically suppressed proportional to $m_H^2/(4\pi v)^2$, compared to a value that would saturate the unitarity bounds. In practice (cf. Fig. 1), the suppression in the differential cross section is an order of magnitude, and the formally subleading transversal degrees of freedom dominate the observable cross section. Thus, we take the SM contribution to the Goldstone-scattering amplitudes as zero. Nonzero contributions are induced by the anomalous operators, which thus become leading. (The spin eigenamplitudes $\mathcal{A}$ have to be normalized by $a_0 = \frac{\mathcal{A}}{32\pi}$.)

$$\mathcal{A}(w^+w^+ \to w^+w^+) = \frac{1}{4}F_{S,0}(2s^2+t^2+u^2) + \frac{1}{2}F_{S,1}(t^2+u^2) - \left(F_{HD}^2\frac{v^2}{4}+F_{HD}\right)\left(\frac{t^2}{t-m_H^2}+\frac{u^2}{u-m_H^2}\right), \quad (33)$$

$$\mathcal{A}(w^+z \to w^+z) = \frac{1}{4}F_{S,0}(s^2+u^2) + \frac{1}{2}F_{S,1}t^2 - \left(F_{HD}^2\frac{v^2}{4}+F_{HD}\right)\frac{t^2}{t-m_H^2}, \quad (34)$$

$$\mathcal{A}(w^+w^- \to w^+w^-) = \frac{1}{4}F_{S,0}(s^2+t^2+2u^2) + \frac{1}{2}F_{S,1}(s^2+t^2) - \left(F_{HD}^2\frac{v^2}{4}+F_{HD}\right)\left(\frac{s^2}{s-m_H^2}+\frac{t^2}{t-m_H^2}\right), \quad (35)$$

$$\mathcal{A}(w^+w^- \to zz) = \frac{1}{4}F_{S,0}(t^2+u^2) + \frac{1}{2}F_{S,1}s^2 - \left(F_{HD}^2\frac{v^2}{4}+F_{HD}\right)\frac{s^2}{s-m_H^2}, \quad (36)$$

$$\mathcal{A}(zz \to zz) = \frac{1}{2}(F_{S,0}+F_{S,1})(s^2+t^2+u^2) - \left(F_{HD}^2\frac{v^2}{4}+F_{HD}\right)\left(\frac{s^2}{s-m_H^2}+\frac{t^2}{t-m_H^2}+\frac{u^2}{u-m_H^2}\right). \quad (37)$$

Note that $s > m_H^2$ for the observed Higgs boson, so there are actually no poles in the physical region.

In the presence of the Higgs boson, there are also amplitudes that involve external Higgs bosons. In terms of custodial $SU(2)$, the Higgs is a singlet, and there are additional independent amplitudes that involve either two or four Higgs bosons. Realistically, the only experimentally accessible channels are $w^+w^- \to hh$ and $zz \to hh$. These channels provide an independent set of observables, and they should be studied in the context of a larger set of operators. This is beyond the scope of the present paper.

Higgs-pair channels also contribute implicitly to the unitarization condition via backscattering into Goldstones, and thus physical vector bosons. Among the set of operators that we consider in the above example, only the dimension-six term $\mathcal{L}_{HD}$ provides a Higgs-pair contribution. The Standard Model contribution, given the approximations, is equivalent to zero. In the following, we neglect this extra contribution for simplicity. Adding it, we would have to apply a further diagonalization of eigenamplitudes in the isospin-zero channel and unitarize the resulting independent eigenamplitudes. Transforming back to the physical basis, the effective F_{HD} term is slightly more suppressed. However, as we will see in the final plots, the $\mathcal{L}_{HD}$ term is of minor importance anyway. For the purposes of the example, we therefore keep the formulas simple and omit this contribution. In a more complete treatment that applies the unitarization framework to the full set of operators and also unitarizes transversal contributions from these sources, it can be properly incorporated.

Since all operators are $SU(2)_C$ symmetric, we can apply isospin symmetry and crossing symmetry and express all amplitudes in terms of a single master amplitude $A(s,t,u)$ [7],

$$\mathcal{A}(w^+w^- \to zz) = A(s,t,u), \quad (38)$$

$$\mathcal{A}(zz \to zz) = A(s,t,u) + A(t,s,u) + A(u,s,t), \quad (39)$$

$$\mathcal{A}(w^+w^- \to w^+w^-) = A(s,t,u) + A(t,s,u), \quad (40)$$

$$\mathcal{A}(w^+z \to w^+z) = A(t,s,u), \quad (41)$$

$$\mathcal{A}(w^+w^+ \to w^+w^+) = A(t,s,u) + A(u,s,t), \quad (42)$$

and construct the isospin eigenamplitudes $\mathcal{A}_I$,

$$\mathcal{A}_2 = A(t,s,u) + A(u,s,t), \quad (43)$$

$$\mathcal{A}_1 = A(t,s,u) - A(u,s,t), \quad (44)$$

$$\mathcal{A}_0 = 3A(s,t,u) + A(t,s,u) + A(u,s,t). \quad (45)$$

After partial wave decomposition $[t = -s/2(1-\cos\Theta)]$

$$A_{I\ell}(s) = \int_{-s}^{0}\frac{dt}{s}\mathcal{A}_I(s,t,u)P_\ell(\cos\Theta), \quad (46)$$

we obtain the isospin-spin eigenamplitudes,

$$\mathcal{A}_{00} = \frac{1}{6}(7F_{S,0}+11F_{S,1})s^2 - \left(F_{HD}^2\frac{v^2}{4}+F_{HD}\right)\left(\frac{3s^2}{s-m_H^2}+2\mathcal{S}_0(s)\right), \quad (47a)$$

$$\mathcal{A}_{02} = \frac{1}{30}(2F_{S,0}+F_{S,1})s^2 - \left(F_{HD}^2\frac{v^2}{4}+F_{HD}\right)2\mathcal{S}_2(s), \quad (47b)$$

$$\mathcal{A}_{11} = \frac{1}{12}(F_{S,0}-2F_{S,1})s^2 - \left(F_{HD}^2\frac{v^2}{4}+F_{HD}\right)2\mathcal{S}_1(s), \quad (47c)$$

$$\mathcal{A}_{13} = -\left(F_{HD}^2\frac{v^2}{4} + F_{HD}\right)2\mathcal{S}_3(s), \tag{47d}$$

$$\mathcal{A}_{20} = \frac{1}{3}(2F_{S,0} + F_{S,1})s^2 - \left(F_{HD}^2\frac{v^2}{4} + F_{HD}\right)2\mathcal{S}_0(s), \tag{47e}$$

$$\mathcal{A}_{22} = \frac{1}{60}(F_{S,0} + 2F_{S,1})s^2 - \left(F_{HD}^2\frac{v^2}{4} + F_{HD}\right)2\mathcal{S}_2(s), \tag{47f}$$

using the following abbreviations from [18]:

$$\mathcal{S}_0 = m_H^2 + \frac{m_H^4}{s}\log\left(\frac{m_H^2}{s+m_H^2}\right) - \frac{s}{2}, \tag{48a}$$

$$\mathcal{S}_1 = 2\frac{m_H^2}{s} + \frac{m_H^4}{s^2}(2m_H^2 + s)\log\left(\frac{m_H^2}{s+m_H^2}\right) + \frac{s}{6}, \tag{48b}$$

$$\mathcal{S}_2 = \frac{m_H^4}{s^2}(6m_H^2 + 3s) + \frac{m_H^4}{s^3}(6m_H^4 + 6m_H^2 s + s^2)\log\left(\frac{m_H^2}{s+m_H^2}\right). \tag{48c}$$

Expressed in terms of the isospin-spin eigenstates, the Goldstone scattering matrix becomes diagonal. It is now straightforward to apply the T-matrix unitarization scheme (equivalent to the K-matrix scheme at this order) to the diagonal isospin-spin eigenamplitudes. For each $I\ell$ combination, the T-matrix unitarized amplitude is given by [cf. (28)]

$$\hat{\mathcal{A}}_{I\ell}(s) = \frac{1}{\mathrm{Re}(\frac{1}{\mathcal{A}_{I\ell}(s)}) - \frac{i}{32\pi}}. \tag{49}$$

We split off the original amplitude $\mathcal{A}_{I\ell}$ that corresponds to the naive EFT and obtain the unitarization correction as

$$\Delta\mathcal{A}_{I\ell} = \hat{\mathcal{A}}_{I\ell} - \mathcal{A}_{I\ell}. \tag{50}$$

Given this set of corrections, we dress the eigenamplitude corrections by the appropriate Legendre polynomials and revert the basis from isospin eigenstates to w^+, z, w^-, so we arrive at counterterms for the individual Goldstone scattering channels,

$$\Delta\mathcal{A}(w^+w^+ \to w^+w^+) = \Delta\mathcal{A}_{20}(s) - 10\Delta\mathcal{A}_{22}(s) + 15\Delta\mathcal{A}_{22}(s)\frac{t^2+u^2}{s^2}, \tag{51}$$

$$\Delta\mathcal{A}(w^+w^- \to zz) = \frac{1}{3}(\Delta\mathcal{A}_{00}(s) - \Delta\mathcal{A}_{20}(s)) - \frac{10}{3}(\Delta\mathcal{A}_{02}(s) - \Delta\mathcal{A}_{22}(s)) + 5(\Delta\mathcal{A}_{02}(s) - \Delta\mathcal{A}_{22}(s))\frac{t^2+u^2}{s^2}, \tag{52}$$

$$\Delta\mathcal{A}(w^+z \to w^+z) = \frac{1}{2}\Delta\mathcal{A}_{20}(s) - 5\Delta\mathcal{A}_{22}(s) + \left(-\frac{3}{2}\Delta\mathcal{A}_{11}(s) + \frac{15}{2}\Delta\mathcal{A}_{22}(s)\right)\frac{t^2}{s^2} + \left(\frac{3}{2}\Delta\mathcal{A}_{11}(s) + \frac{15}{2}\Delta\mathcal{A}_{22}(s)\right)\frac{u^2}{s^2}, \tag{53}$$

$$\Delta\mathcal{A}(w^+w^- \to w^+w^-) = \frac{1}{6}(2\Delta\mathcal{A}_{00}(s) + \Delta\mathcal{A}_{20}(s)) - \frac{5}{3}(2\Delta\mathcal{A}_{02}(s) + \Delta\mathcal{A}_{22}(s)) + \left(5\Delta\mathcal{A}_{02}(s) - \frac{3}{2}\Delta\mathcal{A}_{11}(s) + \frac{5}{2}\Delta\mathcal{A}_{22}(s)\right)\frac{t^2}{s^2} + \left(5\Delta\mathcal{A}_{02}(s) + \frac{3}{2}\Delta\mathcal{A}_{11}(s) + \frac{5}{2}\Delta\mathcal{A}_{22}(s)\right)\frac{u^2}{s^2}, \tag{54}$$

$$\Delta\mathcal{A}(zz \to zz) = \frac{1}{3}(\Delta\mathcal{A}_{00}(s) + 2\Delta\mathcal{A}_{20}(s)) - \frac{10}{3}(\Delta\mathcal{A}_{02}(s) + 2\Delta\mathcal{A}_{22}(s)) + 5(\Delta\mathcal{A}_{02}(s) + 2\Delta\mathcal{A}_{22}(s))\frac{t^2+u^2}{s^2}. \tag{55}$$

Since there are no branch cuts in lowest order, crossing symmetry implies that the amplitude $\mathcal{A}(w^+z \to w^+z)$ in (41) can be obtained from $\mathcal{A}(w^+w^- \to zz)$ in (38) by an exchange of s with t and $\mathcal{A}(w^+w^+ \to w^+w^+)$ in (42) from $\mathcal{A}(w^+w^- \to w^+w^-)$ in (40) by an exchange of s with u [using $A(s,t,u) = A(s,u,t)$]. In the presence of branch cuts, however, there are contributions like resonance poles on the unphysical Riemann sheet that must be nonzero only if the Mandelstam variable is above the threshold M_{thr}^2 of the corresponding branch cut. The resulting factors $\Theta(s - M_{\mathrm{thr}}^2)$ and additional terms proportional to $\Theta(t - M_{\mathrm{thr}}^2)$ and $\Theta(u - M_{\mathrm{thr}}^2)$ have been suppressed in (51)–(55), with the understanding that these formulas will be used only in the case $s > 0 \wedge t < 0 \wedge u < 0$.

As a toy example for this phenomenon, consider a unitarity-violating amplitude

$$\mathcal{A}(s) = \alpha\frac{s}{v^2} \tag{56}$$

resulting from a local dimension-six operator that can be unitarized by replacing the local operator by a resonance exchange

$$\mathcal{A}_R(s) = -\frac{s}{s - M^2 + \mathrm{i}\Gamma M\Theta(s - M^2_{\mathrm{thr}})} \tag{57}$$

with $M^2 = v^2/\alpha$, so that $\mathcal{A}(s)$ and $\mathcal{A}_R(s)$ agree in the region $s \ll M^2$. Since the amplitude must not have a pole with a nonvanishing imaginary part on the physical Riemann sheet, any such pole is located on the second sheet, which can be reached via a branch cut corresponding to an open decay channel of the resonance [114]. Therefore the pole of the crossed amplitude in the t channel

$$\bar{\mathcal{A}}_R(t) = -\frac{t}{t - M^2 + \mathrm{i}\Gamma M\Theta(t - M^2_{\mathrm{thr}})} \tag{58}$$

must not have the imaginary part, because there is no branch cut for $t < 0$ providing access to the second sheet. In (57) and (58), this is expressed by the Θ distributions multiplying the widths.

The analogous analytical structure is found by rewriting the K-matrix unitarized amplitude

$$\mathcal{A}_K(s) = \frac{\alpha s/v^2}{1 - \mathrm{i}\alpha s/v^2} \tag{59}$$

as

$$\mathcal{A}_K(s) = \frac{\mathrm{i}s}{s + \mathrm{i}M^2} \tag{60}$$

to make the existence of a similar pole off the real axis explicit. Again, such a pole must not be located on the physical Riemann sheet, and we may replace $\mathcal{A}(s)$ by $\mathcal{A}_K(s)$ only for $s > 0$, where a nearby branch cut can act as a portal to the second sheet, as shown in Fig. 7. Note that this prescription manifestly unitarizes all partial wave amplitudes for $s \to \infty$, even though the amplitude as a function of s and t appears to rise for $t \to -s$ for each fixed s. The consistency of the analytical structure illustrated in Fig. 7 can also be seen in a perturbative example: in [101] it has been shown explicitly for the example of the O($2N$) model with large N that the K-matrix prescription (60) reproduces the exact amplitude when resummed to all orders.

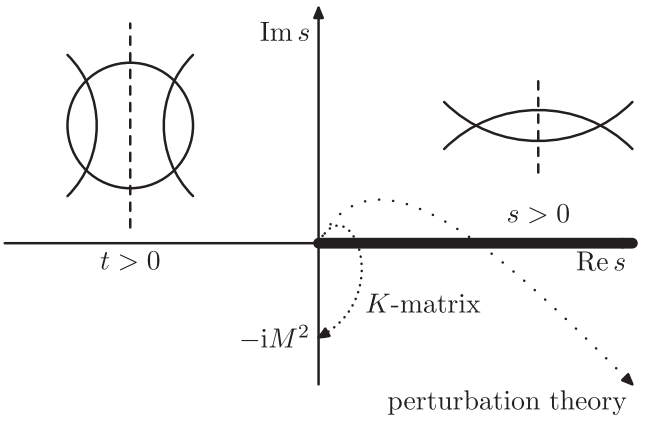

FIG. 7. The analytic structure of resummed scattering amplitudes. As illustrated by the Feynman diagrams, the left-handed (i.e., $t > 0$ or $s < 0$) cut will in general belong to a different channel (i.e., combination of quantum numbers) than the right-handed cut. The diagrams also illustrate that the left-handed cut can appear in a different order of the perturbative expansion than the right-handed cut. Following [101], we also compare the location of the pole in the K-matrix scattering amplitude (60) to the perturbative result. Note that the passage through the region with Im$s > 0$ has been exaggerated for illustrative purposes (cf. [114]). In reality, the pole immediately crosses over to the second sheet.

C. Complete electroweak processes

So far, we have only considered Goldstone-scattering amplitudes, which represent longitudinal vector bosons at asymptotically high energy. The result of the unitarization procedure is a set of correction terms that depend on s, t, u. We would like to use the expressions in a calculation of vector-boson scattering amplitudes at finite energy. To achieve this, we note that by construction, the counterterms have a t and u dependence that is equivalent to the anomalous quartic terms that we started with. We can therefore unambiguously distribute the new contributions among the two different gauge-invariant interaction operators (counterterms) $\mathcal{L}_{S,0}$ and $\mathcal{L}_{S,1}$ that are already present. The algorithm follows precisely the derivation in [18].

In the result, all three parameters $F_{HD}, F_{S,0}, F_{S,1}$ enter both of the counterterm prefactors, respectively. The unitarization procedure effectively modifies and mixes the EFT operator coefficients in a nonlinear way.

We finally switch back from covariant gauge to unitarity gauge and obtain Feynman rules for physical vector bosons. Inserting external momenta and polarization vectors (or fermionic currents), the asymptotic amplitude expressions receive finite low-energy corrections that are related to the W and Z masses, some of them breaking the custodial symmetry.

In the context of complete scattering amplitudes, the new Feynman rules for quartic gauge-boson couplings are evaluated off-shell. We have to define a prescription that determines the energy value in the operator coefficient. Relying on the assumption that the effective vertices are evaluated for an approximately on-shell $2 \to 2$ scattering kinematics, we define the energy value as the square root of the initial- or final-state invariant mass, i.e., the $\sqrt{\hat{s}}$ value for the VV system, represented by their decay products. This completes the algorithm.

Before we turn to concrete results, we should review the assumptions and approximations on which the algorithm is based. First of all, we started from the linear Higgs EFT as the low-energy approximation and assume the absence of new states (resonances) within the accessible energy range.

We have to accept the fact that the model enters a strongly interacting regime, so beyond the threshold where the corrections start to play a role, the prediction becomes a rather uncertain estimate, controlled just by the unitarity requirement. However, the unitarized cross section asymptotically falls off, so the energy range beyond this threshold is again suppressed in the event sample. Finally, the unitarization corrections are strictly valid only in the high-energy limit and for on-shell longitudinal vector bosons in the kinematical configuration of quasielastic scattering. We thus have to require that these conditions are approximately met, typically by imposing vector boson fusion (VBF) cuts in the analysis.

Anomalous interactions of transversal vector bosons would also require unitarization. They can be incorporated, analyzing them in the high-energy limit where they are decoupled from Goldstone bosons and then applying the same scheme to the corrected amplitudes. However, we do not attempt this explicitly in the present paper.

These constraints imply, in particular, that the results *cannot* be applied to the analogous process of triple vector boson production. The SM and any underlying UV completion would allow us to determine the correct analytic structure and relations between processes that are related by crossing external particles between the incoming and outgoing states. However, the unitarization corrections in the present model apply only to s-channel kinematics in $2 \to 2$ scattering and must not be used for the kinematical configuration of triple-boson production where the initial vector boson is far off shell. We may compare this situation to the resummation of the propagator of an unstable particle that may also occur in the t channel. In the context of SM gauge invariance, it is necessary to include extra diagrams in the unitarized result [115]. In the present case where the complete theory is not even known, the corresponding ambiguity is an indication of the unavoidable model dependence of the unitarization procedure.

D. Numerical results: On shell

We have implemented the Feynman rules that correspond to the energy-dependent counterterm operators, as described in the preceding section, in the Monte Carlo event generator WHIZARD [76–78].[2] This allows us to numerically compute unitarized cross sections and generate corresponding event samples at colliders.

We note that up to the perturbative order that we are calculating, there is no difference between the T-matrix and K-matrix unitarization prescriptions. A difference would show up for higher-order or model-specific amplitudes that initially contain an imaginary part.

[2]Note that it is not possible to use an automated tool for Feynman rules to include these rules (as, e.g., via [116]) as one also needs a prescription to single out s channels.

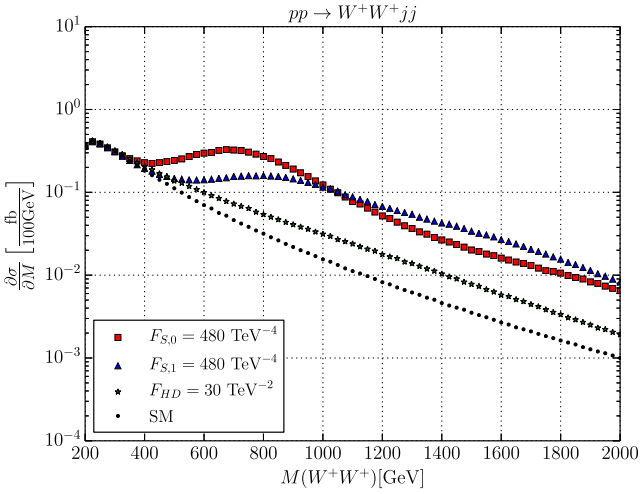

FIG. 8 (color online). $pp \to W^+W^+jj$, unitarized (QCD contributions neglected). Cuts: $M_{jj} > 500$ GeV; $\Delta\eta_{jj} > 2.4$; $p_T^j > 20$ GeV; $|\eta_j| < 4.5$.

The results in Figs. 8,9,10, and 11 are complementary to Fig. 1. They display the unitarized distribution of the VV invariant mass for the same selected values of the parameters $F_{HD}, F_{S,0}, F_{S,1}$, again calculated for the LHC configuration with $\sqrt{s} = 14$ TeV and standard cuts, dijet invariant mass $M_{jj} > 500$ GeV, jet rapidity distance $\Delta\eta_{jj} > 2.4$, a minimal jet transverse momentum of $p_T > 20$ GeV, and a minimal (and opposite) jet rapidity of $|\eta_j| < 4.5$. We show the distinct final states W^+W^+, W^+W^-, W^+Z, and ZZ with the final-state vector bosons taken on shell.

The plots clearly indicate that the naively calculated numbers with anomalous couplings and no unitarization grossly overshoot the more realistic T-matrix results. For

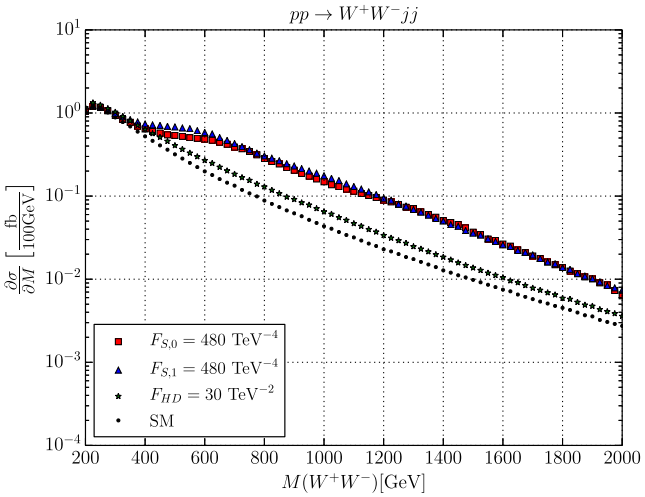

FIG. 9 (color online). $pp \to W^+W^-jj$, unitarized (QCD contributions neglected). Cuts: $M_{jj} > 500$ GeV; $\Delta\eta_{jj} > 2.4$; $p_T^j > 20$ GeV; $|\eta_j| < 4.5$.

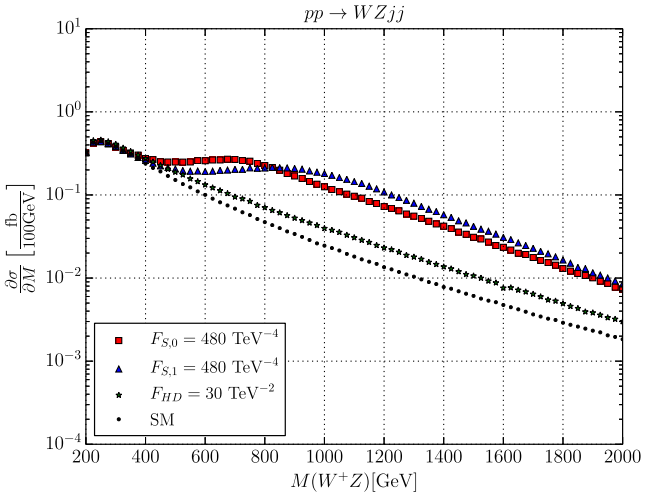

FIG. 10 (color online). $pp \to W^+Zjj$, unitarized (QCD contributions neglected). Cuts: $M_{jj} > 500$ GeV; $\Delta\eta_{jj} > 2.4$; $p_T^j > 20$ GeV; $|\eta_j| < 4.5$.

the chosen parameters, the effect of the dimension-eight operators is more pronounced than the effect of the anomalous Higgs coupling, a dimension-six operator. In all channels, the unitarized curves fall down with energy with the same rate as the SM curves, but enhanced by about one order of magnitude. There is a distinct threshold region where the cross section interpolates between the SM curve and the saturated limit. Only within this small window could a pure EFT description be meaningful.

E. Numerical results: Full processes

At the LHC, the actual final state consists of six fermions, namely two forward jets and the decay products

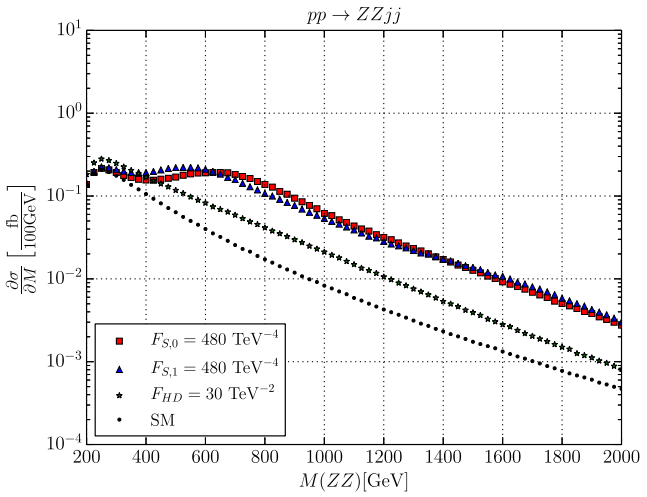

FIG. 11 (color online). $pp \to ZZjj$, unitarized (QCD contributions neglected). Cuts: $M_{jj} > 500$ GeV; $\Delta\eta_{jj} > 2.4$; $p_T^j > 20$ GeV; $|\eta_j| < 4.5$.

of the vector bosons. We present results for the process with same-sign charged leptons,

$$pp \to e^+\mu^+\nu_e\nu_\mu jj, \tag{61}$$

including the complete irreducible background. The events have been generated on the basis of the complete tree-level amplitude that connects the initial and final states. The plots show an unweighted partonic event sample that corresponds to 1 ab^{-1} at the nominal LHC energy of 14 TeV. We have applied standard VBF cuts, as listed in the figure captions.

In Fig. 12, we show the scalar sum of transverse momentum and the azimuthal distance of the charged lepton pair, respectively. Both observables are sensitive to the chosen values of the anomalous couplings. There is a significant difference between the SM prediction (blue/dark regions) and the prediction with nonzero operator coefficient and unitarization (red/medium regions). For reference, we also display the unphysical results that we would generate without unitarization (yellow/light regions).

All numbers have been calculated with the WHIZARD event generator [76] in version 2.2, which implements the T-matrix unitarized model with dimension-six and dimension-eight operators, as explained above.

V. SUMMARY AND CONCLUSION

We have developed a method to model the high-energy behavior of quasielastic vector-boson scattering processes in a way that it can be applied to collider analyses, covering in particular hadron colliders where observables cannot always be limited to a narrow energy range. The method interpolates between the SM with a light Higgs boson as the low-energy limit, its effective-theory extension, and a high-energy behavior that remains consistent with unitarity constraints.

It turns out that the only experimentally distinguishable possibilities for vector-boson scattering processes are (i) the pure SM, (ii) new particles, as, e.g., in a two-Higgs doublet model, and (iii) a deviation that smoothly increases with energy and indicates a strongly interacting Higgs sector. We study the latter possibility. Small deviations that stay within the weakly interacting regime are mostly indistinguishable from the SM, at least in vector boson scattering.

In this work we do not propose any concrete model beyond the SM. However, for quantitatively establishing the validity of the SM, or for qualifying the significance of any possible experimental discrepancy, we need an EFT approach that provides parametrizations for deviations in all possible directions in model space. For being phenomenologically useful, such alternative parametrizations must be consistent with unitarity as a limitation to the number of events that can reasonably contribute to a particular observable.

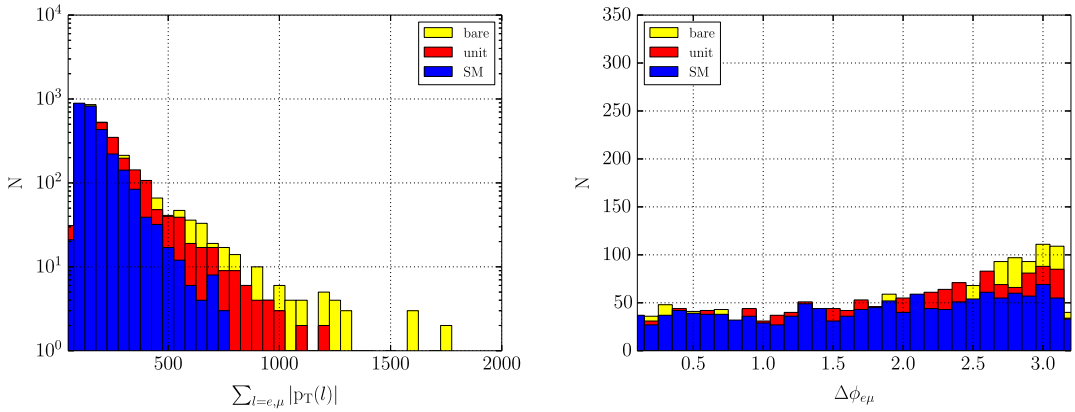

$F_{HD} = 30\ \mathrm{TeV}^{-2}$

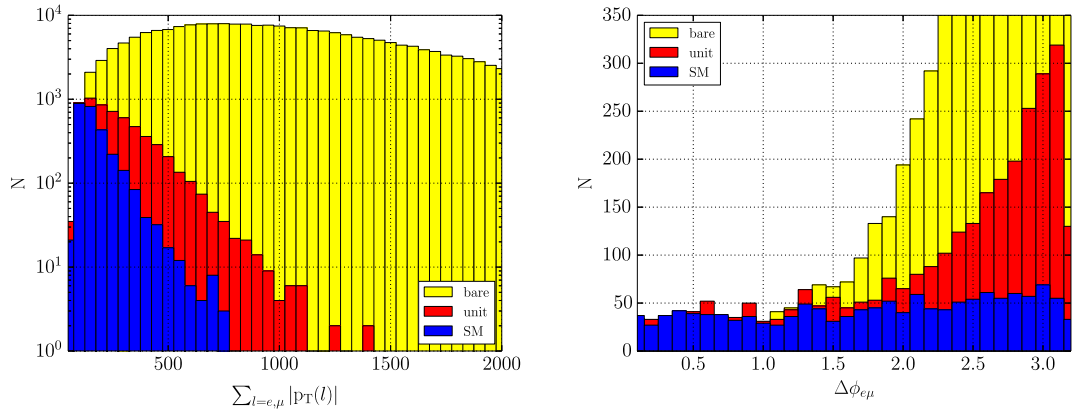

$F_{S,0} = 480\ \mathrm{TeV}^{-4}$

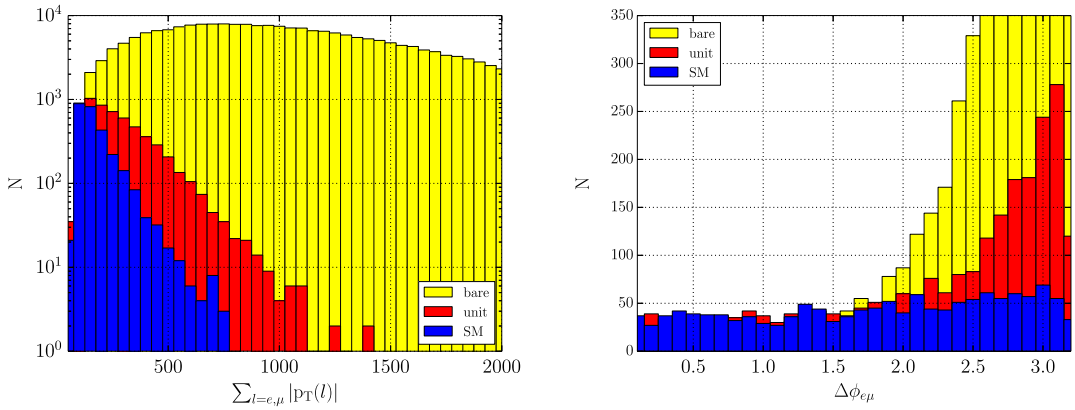

$F_{S,1} = 480\ \mathrm{TeV}^{-4}$

FIG. 12 (color online). $pp \to e^+\mu^+\nu_e\nu_\mu jj$, $\sqrt{s} = 14$ TeV, L $= 1000$ fb^{-1}. Cuts: $M_{jj} > 500$ GeV; $\Delta\eta_{jj} > 2.4$; $p_T^j > 20$ GeV; $|\eta_j| < 4.5$; $p_T^\ell > 20$ GeV.

The problem of modeling high-energy electroweak interactions has already been discussed three decades ago when multi-TeV colliders were planned for the first time. However, the present context is somewhat different: a reasonable model must smoothly interpolate high-energy strong interactions with the now-established *light*-Higgs scenario. Adapting methods originally developed for the Higgs-less case, we propose to unitarize the EFT amplitudes by extending the parameter-free K-matrix formalism. We reformulate this method as a direct T-matrix scheme,

such that it unitarizes any given model without requiring a perturbative expansion or introducing additional structure in the result. We have described this approach in detail, including the systematic embedding of the new effects in the machinery of Monte Carlo simulation for the full multifermion processes.

The underlying T-matrix prescription ensures that any computed results do not overshoot the physical limit, but it does not have any further physical interpretation. Given sufficient experimental precision, we should get a handle on the behavior of the invariant-mass distribution beyond the maximum that is related to the strong-interaction threshold. Possibilities for modeling VBS beyond this threshold have been sketched in [11,12] and will be developed in more detail in a separate paper [117].

ACKNOWLEDGMENTS

We acknowledge enlightening discussions and helpful input from Philipp Anger, Carsten Bittrich, Tao Han, Michael Kobel, Ashutosh Kotwal, Marc-André Pleier, Ulrike Schnoor, and Anja Vest. T. O. is supported by Bundesministerium für Bildung und Forschung, J. R. R. has been partially supported by the Strategic Helmholtz Alliance "Physics at the Terascale" of the Helmholtz Alliance.

APPENDIX A: NOTATIONAL CONVENTIONS

The field content of the EFT is given by fermions, gluons, electroweak vector bosons, and the Higgs doublet, which in a linear gauge consists of the physical Higgs boson and three Goldstone bosons w^+, w^-, w^3. We do not write fermions or gluons explicitly. For electroweak gauge bosons, we define

$$\mathbf{D}_\mu \mathbf{H} = \partial_\mu \mathbf{H} - \mathrm{i}g \mathbf{W}_\mu \mathbf{H} - \mathrm{i}g' \mathbf{H} \mathbf{B}_\mu, \tag{A1}$$

$$\mathbf{W}_{\mu\nu} = \partial_\mu \mathbf{W}_\nu - \partial_\nu \mathbf{W}_\mu - \mathrm{i}g[\mathbf{W}_\mu, \mathbf{W}_\nu], \tag{A2}$$

$$\mathbf{B}_{\mu\nu} = \partial_\mu \mathbf{B}_\nu - \partial_\nu \mathbf{B}_\mu, \tag{A3}$$

with

$$\mathbf{W}_\mu = W_\mu^a \frac{\tau^a}{2}, \qquad \mathbf{B}_\mu = -\frac{\tau^3}{2} B_\mu. \tag{A4}$$

In the linear representation, the SM Higgs field combines with the Goldstone bosons as an electroweak doublet. The Higgs sector has an additional global $SU(2)_C$ (custodial) symmetry [73]. To make the $SU(2)_C$ transformation properties explicit, we parametrize the Higgs field as the Hermitian matrix

$$\mathbf{H} = \frac{1}{2} \begin{pmatrix} v + h - \mathrm{i}w^3 & -\mathrm{i}\sqrt{2} w^+ \\ -\mathrm{i}\sqrt{2} w^- & v + h + \mathrm{i}w^3 \end{pmatrix}. \tag{A5}$$

The physical Higgs field multiplies the unit matrix, while the Goldstone bosons w^+, w^3, w^- are the components proportional to the Pauli matrices τ^+, τ^3, τ^-. $SU(2)_L$ transformations U_L, $SU(2)_R$ transformations U_R, and custodial $SU(2)_C$ transformations U_C act as

$$\mathbf{H} \to U_L \mathbf{H}, \qquad \mathbf{H} \to \mathbf{H} U_R^\dagger, \qquad \mathbf{H} \to U_C \mathbf{H} U_C^\dagger, \tag{A6}$$

respectively. The τ^3 part of $SU(2)_R$ coincides with hypercharge $U(1)_Y$ transformations, while $\tau^{1,2}$-associated transformations are not realized as local gauge symmetries. Under custodial trunsformations, the Higgs field decomposes into singlet (the physical Higgs) and triplet (Goldstones). Conversely, under $SU(2)_L$ gauge transformations, the two columns of the Higgs matrix transform independently as the conventional complex doublet Φ and its charge conjugate. In unitarity gauge, the Goldstone bosons disappear, and the matrix reduces to the $v + h$ term.

The bosonic part of the lowest order EFT, i.e., the plain SM Lagrangian, reads

$$\mathcal{L}_{\mathrm{min}} = -\frac{1}{2} \mathrm{tr}[\mathbf{W}_{\mu\nu} \mathbf{W}^{\mu\nu}] - \frac{1}{2} \mathrm{tr}[\mathbf{B}_{\mu\nu} \mathbf{B}^{\mu\nu}] \tag{A7}$$

$$+ \mathrm{tr}[(\mathbf{D}_\mu \mathbf{H})^\dagger \mathbf{D}^\mu \mathbf{H}] + \mu^2 \mathrm{tr}[\mathbf{H}^\dagger \mathbf{H}] - \frac{\lambda}{2} (\mathrm{tr}[\mathbf{H}^\dagger \mathbf{H}])^2. \tag{A8}$$

For a precise definition of higher-dimensional operators, we have to express the free parameters of the EFT, order by order in the operator dimension, in terms of observable quantities. A possible choice for such a renormalization scheme, applicable to the operator expansion at tree level and beyond, is

$$g = 2\frac{m_W}{v}, \qquad g' = 2\frac{\sqrt{m_Z^2 - m_W^2}}{v},$$
$$\mu^2 = \frac{1}{2} m_H^2, \qquad \lambda = \frac{m_H^2}{v^2}, \tag{A9}$$

for the parameters in the SM Lagrangian, (A7), with particle masses and the Higgs vacuum expectation value v as fixed input. In particular, the definition of g and g' unambiguously determines the covariant field strength and the covariant derivative that we use for constructing higher-dimensional operators. Furthermore, we may fix the kinetic-energy normalization to their conventional SM values.

We have deliberately excluded fermions here. Light fermions are coupled by gauge bosons. For our purposes, they act like external currents and are properly taken into account when the unitarized amplitudes are embedded into the full process. Heavy fermions are important in the context of Higgs physics, but absent from the initial state. In the final state, they are identifiable. Here, we just consider processes that ultimately involve light fermions.

In passing, we note that genuine anomalous interactions of light fermions are experimentally accessible in processes such as lepton and jet pair production.

APPENDIX B: UNITARIZATION, *K* MATRIX, AND ALL THAT: PROOFS

1. Non-Hermitian *K* matrix

If the K matrix is not Hermitian, we need to find a generalization of (6), i.e.,

$$T = \frac{K'}{\mathbf{1} - \mathrm{i}K'/2}, \tag{B1}$$

with a suitable K'. The most straightforward approach is to just throw away the imaginary parts $K' = \mathrm{Re}K = (K + K^\dagger)/2$. The interpretation of the Cayley transform as an inverse stereographic projection suggests a less drastic approach that retains the imaginary part. Consider the family $\{K_\kappa\}$ of K matrices that have the same projection with center $\mathrm{i}\mathbf{1}$,

$$\frac{K_\kappa}{2} - \mathrm{i}\mathbf{1} = \kappa\left(\frac{K}{2} - \mathrm{i}\mathbf{1}\right)\kappa, \tag{B2a}$$

$$\kappa^\dagger = \kappa > 0, \tag{B2b}$$

and choose the unique self-adjoint member $K' \in \{K_\kappa\}$ of this family

$$K' = (K')^\dagger. \tag{B2c}$$

As long[3] as $\mathrm{Im}K/2 < \mathbf{1}$, there is a unique solution with a converging power series expansion

$$\kappa = \frac{1}{\sqrt{\mathbf{1} - \mathrm{Im}K/2}}, \tag{B4a}$$

$$K' = \kappa(\mathrm{Re}K)\kappa, \tag{B4b}$$

resulting in

$$T = \kappa(\mathrm{Re}K)\frac{1}{\mathbf{1} - \mathrm{i}K^\dagger/2}\kappa^{-1} = \kappa^{-1}\frac{1}{\mathbf{1} - \mathrm{i}K^\dagger/2}(\mathrm{Re}K)\kappa. \tag{B5}$$

[3]We can use the Riesz-Dunford functional calculus [91–93] to construct projectors on subspaces corresponding to parts of the spectrum of $\mathrm{Im}K/2$

$$P_\Sigma = \int_{\partial\Sigma}\frac{\mathrm{d}z}{2\pi\mathrm{i}}\frac{1}{z\mathbf{1} - \mathrm{Im}K/2}, \tag{B3}$$

where Σ contains the desired part of the spectrum of $\mathrm{Im}K/2$.

For normal K, i.e., $KK^\dagger = K^\dagger K$, everything commutes, and we may write

$$T = \frac{\mathrm{Re}K}{\mathbf{1} - \mathrm{i}K^\dagger/2} = \frac{\mathrm{Re}K}{\mathbf{1} - \mathrm{i}\mathrm{Re}K/2 - \mathrm{Im}K/2}$$

instead, highlighting the contribution of $\mathrm{Im}K = (K - K^\dagger)/2\mathrm{i}$.

2. Properties of *T*-matrix unitarized (linear projection) operators

The unitarity of the S matrix, $SS^\dagger = S^\dagger S = 1$, implies that each interaction matrix, $S = 1 + iT$, has to satisfy

$$\mathrm{T}^\dagger\mathrm{T} = -\mathrm{i}(\mathrm{T} - \mathrm{T}^\dagger). \tag{B6}$$

For T-matrix unitarized operators (19) via linear projection, we use

$$\mathrm{T}(\mathrm{T}_0) = \frac{\mathrm{Re}\mathrm{T}_0}{\mathbb{1} - \frac{\mathrm{i}}{2}\mathrm{T}_0^\dagger} = \frac{\mathrm{Re}\mathrm{T}_0}{\mathbb{1} + \frac{1}{4}\mathrm{T}_0\mathrm{T}_0^\dagger}\left(\mathbb{1} + \frac{\mathrm{i}}{2}\mathrm{T}_0\right) \tag{B7}$$

to show the unitarity of the corresponding S operator,

$$\begin{aligned}\mathrm{S}\mathrm{S}^\dagger &= \mathbb{1} - 2\mathrm{Im}(T) + \mathrm{T}\mathrm{T}^\dagger \\ &= \mathbb{1} - \frac{(\mathrm{Re}\mathrm{T}_0)^2}{\mathbb{1} + \frac{1}{4}\mathrm{T}_0\mathrm{T}_0^\dagger} + \frac{(\mathrm{Re}\mathrm{T}_0)^2}{\mathbb{1} + \frac{1}{4}\mathrm{T}_0\mathrm{T}_0^\dagger} = \mathbb{1}.\end{aligned} \tag{B8}$$

In the same way, we can show the idempotency of the T operation,

$$\begin{aligned}\mathrm{T}(\mathrm{T}(\mathrm{T}_0)) &= \frac{\mathrm{Re}\mathrm{T}(\mathrm{T}_0)}{1 - \frac{\mathrm{i}}{2}\mathrm{T}(\mathrm{T}_0)^\dagger} = \frac{\frac{\mathrm{Re}\mathrm{T}_0}{\mathbb{1} + \frac{1}{4}\mathrm{T}_0\mathrm{T}_0^\dagger}(\mathbb{1} - \frac{1}{2}\mathrm{Im}\mathrm{T}_0)}{\mathbb{1} - \frac{\mathrm{i}}{2}\frac{\mathrm{Re}\mathrm{T}_0(\mathbb{1} - \frac{\mathrm{i}}{2}\mathrm{T}_0^\dagger)}{(\mathbb{1} - \frac{\mathrm{i}}{2}\mathrm{T}_0^\dagger)(\mathbb{1} + \frac{\mathrm{i}}{2}\mathrm{T}_0)}} \\ &= \frac{\mathrm{Re}\mathrm{T}_0}{\mathbb{1} + \frac{1}{4}\mathrm{T}_0\mathrm{T}_0^\dagger}\left(\mathbb{1} + \frac{\mathrm{i}}{2}\mathrm{T}_0\right) = \mathrm{T}(\mathrm{T}_0).\end{aligned} \tag{B9}$$

3. Properties of *T*-matrix unitarized (Thales projection) operators

In this section we take the definition of the T-matrix unitarized operator from (29) and show, using

$$\mathrm{T}(\mathrm{T}_0) = \frac{1}{\mathrm{Re}(\frac{1}{\mathrm{T}_0}) - \frac{\mathrm{i}}{2}\mathbb{1}} = \frac{1}{\mathrm{Re}(\frac{1}{\mathrm{T}_0})^2 + \frac{1}{4}\mathbb{1}}\left(\mathrm{Re}\left(\frac{1}{\mathrm{T}_0}\right) + \frac{\mathrm{i}}{2}\mathbb{1}\right), \tag{B10}$$

the unitarity of the corresponding S operator,

$$SS^\dagger = \mathbb{1} - 2\mathrm{Im}(T) + TT^\dagger = \mathbb{1} - \frac{1}{\mathrm{Re}(\frac{1}{T_0})^2 + \frac{1}{4}\mathbb{1}} + \frac{1}{\mathrm{Re}(\frac{1}{T_0})^2 + \frac{1}{4}\mathbb{1}} = \mathbb{1}. \quad \text{(B11)}$$

Also, it is easy to see that this operation is idempotent,

$$T(T(T_0)) = \frac{1}{\mathrm{Re}(\frac{1}{T(T_0)}) - \frac{i}{2}\mathbb{1}} = \frac{1}{\mathrm{Re}(\mathrm{Re}(\frac{1}{T_0}) - \frac{i}{2}\mathbb{1}) - \frac{i}{2}\mathbb{1}} = \frac{1}{\mathrm{Re}(\frac{1}{T_0}) - \frac{i}{2}\mathbb{1}} = T(T_0). \quad \text{(B12)}$$

APPENDIX C: OPERATOR BASES AND THEIR TRANSLATION

1. Introduction to different sets of operator bases

It has become customary to write the EFT operator basis in a form that is algebraically simple, so each basic operator is a single monomial of the fields with a single coefficient. For the renormalizable part of the theory, this is justified by the usual renormalization procedure where all terms are renormalized multiplicatively.

There is vast literature on choices of operator bases for dimension-six and dimension-eight operators in the electroweak sector; we only need a sample operator here to demonstrate our point about the unitarization procedure, so we only briefly mention the translation between the nonlinear and linear matrix representations of these operators. An extensive discussion of the operator bases is a different topic and discussed in a follow-up paper [117].

2. Translation between nonlinear and linear matrix representation

We can compare the effective Lagrangians in Appelquist-Alboteanu parametrization

$$\mathcal{L}_4 = \alpha_4 \mathrm{Tr}[\mathbf{V}_\mu \mathbf{V}_\nu]\mathrm{Tr}[\mathbf{V}^\mu \mathbf{V}^\nu],$$
$$\mathcal{L}_5 = \alpha_5 \mathrm{Tr}[\mathbf{V}_\mu \mathbf{V}^\mu]\mathrm{Tr}[\mathbf{V}_\nu \mathbf{V}^\nu]$$

from [18,20] in unitarity gauge

$$\mathbf{V}_\mu \hat{=} -\mathrm{i}gW_\mu^a \frac{\tau^a}{2} + \mathrm{i}g' B_\mu \frac{\tau^3}{2}$$

to $\mathcal{L}_{S,0}$ and $\mathcal{L}_{S,1}$. Because we are only interested in the VBS part of these two Lagrangians, simplifying the covariant derivative from $\mathcal{L}_{S,0}$ and $\mathcal{L}_{S,1}$ as

$$\mathbf{D}_\mu \mathbf{H} = \frac{v}{2}(-\mathrm{i}g\mathbf{W}_\mu - \mathrm{i}g'\mathbf{B}_\mu) = \frac{v}{2}\left(-\mathrm{i}gW_\mu^a \frac{\tau^a}{2} + \mathrm{i}g' B_\mu \frac{\tau^3}{2}\right) = \frac{v}{2}\mathbf{V}_\mu, \quad \text{(C1)}$$

$$(\mathbf{D}_\mu \mathbf{H})^\dagger = -\frac{v}{2}\mathbf{V}_\mu, \quad \text{(C2)}$$

leads to

$$\mathcal{L}_{S,0} = F_{S,0}\frac{v^4}{16}\mathrm{Tr}[\mathbf{V}_\mu \mathbf{V}_\nu]\mathrm{Tr}[\mathbf{V}^\mu \mathbf{V}^\nu], \quad \text{(C3)}$$

$$\mathcal{L}_{S,1} = F_{S,1}\frac{v^4}{16}\mathrm{Tr}[\mathbf{V}_\mu \mathbf{V}^\mu]\mathrm{Tr}[\mathbf{V}_\nu \mathbf{V}^\nu]. \quad \text{(C4)}$$

Therefore we can relate the coefficients of these different notations,

$$\alpha_4 = F_{S,0}\frac{v^4}{16}, \quad \text{(C5)}$$

$$\alpha_5 = F_{S,1}\frac{v^4}{16}. \quad \text{(C6)}$$

So the coefficients for the operators $\mathcal{L}_{S,0}$ and $\mathcal{L}_{S,1}$ are equivalent to values of α_4 and α_5 of ~ 0.11, which are within the limits from the latest ATLAS analysis [8] ($-0.14 < \alpha_4 < 0.16$ and $-0.23 < \alpha_5 < 0.24$).

APPENDIX D: FEYNMAN RULES

1. Feynman rules from new physics operators

a. $\mathcal{L}_S$

The Lagrangian

$$\mathcal{L}_{S,0} = F_{S,0}\mathrm{tr}[(\mathbf{D}_\mu \mathbf{H})^\dagger \mathbf{D}_\nu \mathbf{H}] \cdot \mathrm{tr}[(\mathbf{D}^\mu \mathbf{H})^\dagger \mathbf{D}^\nu \mathbf{H}], \quad \text{(D1)}$$

$$\mathcal{L}_{S,1} = F_{S,1}\mathrm{tr}[(\mathbf{D}_\mu \mathbf{H})^\dagger \mathbf{D}^\mu \mathbf{H}] \cdot \mathrm{tr}[(\mathbf{D}_\nu \mathbf{H})^\dagger \mathbf{D}^\nu \mathbf{H}], \quad \text{(D2)}$$

leads to the following Feynman rules in the unitarity gauge (neglecting all vertices including a Higgs boson and five or more external fields):

$$W_{\mu_1}^+ W_{\mu_2}^+ W_{\mu_3}^- W_{\mu_4}^- : \frac{\mathrm{i}g^4 v^4}{16}[(F_{S,0} + 2F_{S,1})(g_{\mu_1\mu_3}g_{\mu_2\mu_4} + g_{\mu_1\mu_4}g_{\mu_2\mu_3}) + 2F_{S,0}g_{\mu_1\mu_2}g_{\mu_3\mu_4}], \quad \text{(D3)}$$

$$Z_{\mu_1} Z_{\mu_2} W_{\mu_3}^+ W_{\mu_4}^- : \frac{\mathrm{i}g^4 v^4}{16c_w^2}[F_{S,0}(g_{\mu_1\mu_3}g_{\mu_2\mu_4} + g_{\mu_1\mu_4}g_{\mu_2\mu_3}) + 2F_{S,1}g_{\mu_1\mu_2}g_{\mu_3\mu_4}], \quad \text{(D4)}$$

$$Z_{\mu_1}Z_{\mu_2}Z_{\mu_3}Z_{\mu_4}: \frac{\mathrm{i}g^4v^4}{8c_w^4}(F_{S,0}+F_{S,1})(g_{\mu_1\mu_2}g_{\mu_3\mu_4}+g_{\mu_1\mu_3}g_{\mu_2\mu_4}+g_{\mu_1\mu_4}g_{\mu_2\mu_3}). \tag{D5}$$

b. $\mathcal{L}_{HD}$

The Lagrangian

$$\mathcal{L}_{HD} = F_{HD}\mathrm{tr}\left[\mathbf{H}^\dagger\mathbf{H}-\frac{v^2}{4}\right]\cdot\mathrm{tr}[(\mathbf{D}_\mu\mathbf{H})^\dagger\mathbf{D}_\mu\mathbf{H}] \tag{D6}$$

leads to the following Feynman rules in unitarity gauge (neglecting all vertices with more than one Higgs):

$$hW_\mu^+W_\nu^-: \frac{\mathrm{i}g^2v^3}{4}F_{HD}g_{\mu\nu}, \tag{D7}$$

$$hZ_\mu Z_\nu: \frac{\mathrm{i}g^2v^3}{4s_w^2}F_{HD}g_{\mu\nu}, \tag{D8}$$

2. Feynman rules: Unitarization corrections

These "Feynman rules" are only used for s-channel scattering of $VV\to VV$ with the center-of-mass energy $s=(p_1+p_2)^2$ and counterterms $\mathcal{A}_{ij}$ (50),

$$W_{\mu_1}^\pm W_{\mu_2}^\pm \to W_{\mu_3}^\pm W_{\mu_4}^\pm: \frac{g^4v^4}{4}\left[(\Delta\mathcal{A}_{02}(s)-10\Delta\mathcal{A}_{22}(s))\frac{g_{\mu_1\mu_2}g_{\mu_3\mu_4}}{s^2}+15\Delta\mathcal{A}_{22}(s)\frac{g_{\mu_1\mu_3}g_{\mu_2\mu_4}+g_{\mu_1\mu_4}g_{\mu_2\mu_3}}{s^2}\right], \tag{D9}$$

$$W_{\mu_1}^\pm W_{\mu_2}^\mp \to Z_{\mu_3}Z_{\mu_4}: \frac{g^4v^4}{4c_w^2}\left[\left(\frac{1}{3}(\Delta\mathcal{A}_{00}(s)-\Delta\mathcal{A}_{20}(s))-\frac{10}{3}(\Delta\mathcal{A}_{02}(s)-\Delta\mathcal{A}_{22}(s))\right)\frac{g_{\mu_1\mu_2}g_{\mu_3\mu_4}}{s^2}\right.$$
$$\left.+5(\Delta\mathcal{A}_{02}(s)-\Delta\mathcal{A}_{22}(s))\frac{g_{\mu_1\mu_3}g_{\mu_2\mu_4}+g_{\mu_1\mu_4}g_{\mu_2\mu_3}}{s^2}\right], \tag{D10}$$

$$W_{\mu_1}^\pm Z_{\mu_2}\to W_{\mu_3}^\pm Z_{\mu_4}: \frac{g^4v^4}{4c_w^2}\left[\left(\frac{1}{2}\Delta\mathcal{A}_{20}(s)-5\Delta\mathcal{A}_{22}(s)\right)\frac{g_{\mu_1\mu_2}g_{\mu_3\mu_4}}{s^2}+\left(-\frac{3}{2}\Delta\mathcal{A}_{11}(s)+\frac{15}{2}\Delta\mathcal{A}_{22}(s)\right)\frac{g_{\mu_1\mu_3}g_{\mu_2\mu_4}}{s^2}\right.$$
$$\left.+\left(\frac{3}{2}\Delta\mathcal{A}_{11}(s)+\frac{15}{2}\Delta\mathcal{A}_{22}(s)\right)\frac{g_{\mu_1\mu_4}g_{\mu_2\mu_3}}{s^2}\right], \tag{D11}$$

$$W_{\mu_1}^\pm W_{\mu_2}^\mp \to W_{\mu_3}^\pm W_{\mu_4}^\mp: \frac{g^4v^4}{4}\left[\left(\frac{1}{6}(2\Delta\mathcal{A}_{00}(s)+\Delta\mathcal{A}_{20}(s))-\frac{5}{3}(2\Delta\mathcal{A}_{02}(s)+\Delta\mathcal{A}_{22}(s))\right)\frac{g_{\mu_1\mu_2}g_{\mu_3\mu_4}}{s^2}\right.$$
$$\left.+\left(5\Delta\mathcal{A}_{02}(s)-\frac{3}{2}\Delta\mathcal{A}_{11}(s)+\frac{5}{2}\Delta\mathcal{A}_{22}(s)\right)\frac{g_{\mu_1\mu_3}g_{\mu_2\mu_4}}{s^2}+\left(5\Delta\mathcal{A}_{02}(s)+\frac{3}{2}\Delta\mathcal{A}_{11}(s)+\frac{5}{2}\Delta\mathcal{A}_{22}(s)\right)\frac{g_{\mu_1\mu_4}g_{\mu_2\mu_3}}{s^2}\right], \tag{D12}$$

$$Z_{\mu_1}Z_{\mu_2}\to Z_{\mu_3}Z_{\mu_4}: \frac{g^4v^4}{4c_w^4}\left[\left(\frac{1}{3}(\Delta\mathcal{A}_{00}(s)+2\Delta\mathcal{A}_{20}(s))-\frac{10}{3}(\Delta\mathcal{A}_{02}(s)+2\Delta\mathcal{A}_{22}(s))\right)\frac{g_{\mu_1\mu_2}g_{\mu_3\mu_4}}{s^2}\right.$$
$$\left.+5(\Delta\mathcal{A}_{02}(s)+2\Delta\mathcal{A}_{22}(s))\frac{g_{\mu_1\mu_3}g_{\mu_2\mu_4}+g_{\mu_1\mu_4}g_{\mu_2\mu_3}}{s^2}\right]. \tag{D13}$$

[1] G. Aad *et al.* (ATLAS Collaboration), Observation of a new particle in the search for the Standard Model Higgs boson with the ATLAS detector at the LHC, Phys. Lett. B **716**, 1 (2012).

[2] S. Chatrchyan *et al.* (CMS Collaboration), Observation of a new boson at a mass of 125 GeV with the CMS experiment at the LHC, Phys. Lett. B **716**, 30 (2012).

[3] R. Aleksan *et al.* (European Strategy for Particle Physics Preparatory Group Collaboration), Physics briefing book: Input for the Strategy Group to draft the update of the European Strategy for Particle Physics, http://europeanstrategygroup.web.cern.ch/europeanstrategygroup/Briefing_book.pdf, Report No. CERN-ESG-005.

[4] R. Brock *et al.*, Planning the future of U.S. particle physics (Snowmass 2013): Chapter 3: Energy frontier, arXiv:1401.6081.

[5] C. Degrande *et al.*, Monte Carlo tools for studies of non-standard electroweak gauge boson interactions in multi-boson processes: A Snowmass White Paper, arXiv:1309.7890.

[6] F. Gianotti, Prospects at high energy and luminosity hadron colliders, https://indico.cern.ch/event/275412/session/0/contribution/8.

[7] B. W. Lee, C. Quigg, and H. B. Thacker, The Strength of Weak Interactions at Very High-Energies and the Higgs Boson Mass, Phys. Rev. Lett. **38**, 883 (1977); Weak interactions at very high-energies: The role of the Higgs boson mass, Phys. Rev. D **16**, 1519 (1977).

[8] G. Aad *et al.* (ATLAS Collaboration), Evidence for Electroweak Production of $W^{\pm}W^{\pm}jj$ in pp Collisions at $\sqrt{s} = 8$ TeV with the ATLAS Detector, Phys. Rev. Lett. **113**, 141803 (2014).

[9] CMS Collaboration, Vector boson scattering in a final state with two jets and two same-sign leptons, Report No. CMS-PAS-SMP-13-015, http://cds.cern.ch/record/1713393.

[10] M. Beyer, W. Kilian, P. Křstonošic, K. Mönig, J. Reuter, E. Schmidt, and H. Schröder, Determination of new electroweak parameters at the ILC – Sensitivity to new physics, Eur. Phys. J. C **48**, 353 (2006).

[11] J. Reuter, W. Kilian, and M. Sekulla, Simplified models for new physics in vector boson scattering – Input for Snowmass 2013, arXiv:1307.8170.

[12] J. Reuter, W. Kilian, and M. Sekulla, Simplified models for vector boson scattering at ILC and CLIC, LCWS 2013, University of Tokyo, arXiv:1403.7392.

[13] M. S. Chanowitz and M. K. Gaillard, Multiple production of W and Z as a signal of new strong interactions, Phys. Lett. **142B**, 85 (1984).

[14] M. S. Chanowitz and M. K. Gaillard, The TeV physics of strongly interacting W's and Z's, Nucl. Phys. **B261**, 379 (1985).

[15] M. S. Chanowitz, M. Golden, and H. Georgi, Universal Scattering Theorems for Strongly Interacting W's and Z's, Phys. Rev. Lett. **57**, 2344 (1986).

[16] M. S. Chanowitz, M. Golden, and H. Georgi, Low-energy theorems for strongly interacting W's and Z's, Phys. Rev. D **36**, 1490 (1987).

[17] M. S. Chanowitz and W. Kilgore, Complementarity of resonant and nonresonant strong WW scattering at the LHC, Phys. Lett. B **322**, 147 (1994).

[18] A. Alboteanu, W. Kilian, and J. Reuter, Resonances and unitarity in weak boson scattering at the LHC, J. High Energy Phys. 11 (2008) 010.

[19] S. Weinberg, Nonlinear realizations of chiral symmetry, Phys. Rev. **166**, 1568 (1968).

[20] T. Appelquist and C. W. Bernard, Strongly interacting Higgs bosons, Phys. Rev. D **22**, 200 (1980).

[21] A. C. Longhitano, Heavy Higgs bosons in the Weinberg-Salam model, Phys. Rev. D **22**, 1166 (1980).

[22] S. Dawson and G. Valencia, Chiral Lagrangians and WW scattering, Nucl. Phys. **B352**, 27 (1991).

[23] T. Appelquist and G.-H. Wu, The electroweak chiral Lagrangian and new precision measurements, Phys. Rev. D **48**, 3235 (1993).

[24] A. Dobado, M. J. Herrero, J. R. Pelaez, E. Ruiz Morales, and M. T. Urdiales, Learning about the strongly interacting symmetry breaking sector at LHC, Phys. Lett. B **352**, 400 (1995).

[25] A. Dobado and M. T. Urdiales, Determination of the electroweak chiral Lagrangian parameters at the LHC, Z. Phys. C **71**, 659 (1996).

[26] A. Dobado, A. Gomez-Nicola, A. L. Maroto, and J. R. Pelaez, *Effective Lagrangians for the Standard Model*, Texts and Monographs in Physics (Springer-Verlag, New York, 1997).

[27] W. Kilian, Electroweak symmetry breaking: The bottom-up approach, Springer Tracts Mod. Phys. **198**, 1 (2003).

[28] E. Boos, H. J. He, W. Kilian, A. Pukhov, C. P. Yuan, and P. M. Zerwas, Strongly interacting vector bosons at TeV e^+e^- linear colliders, Phys. Rev. D **57**, 1553 (1998).

[29] E. Boos, H. J. He, W. Kilian, A. Pukhov, C. P. Yuan, and P. M. Zerwas, Strongly interacting vector bosons at TeV e^+e^- linear colliders: Addendum, Phys. Rev. D **61**, 077901 (2000).

[30] A. S. Belyaev, O. J. P. Eboli, M. C. Gonzalez-Garcia, J. K. Mizukoshi, S. F. Novaes, and I. Zacharov, Strongly interacting vector bosons at the CERN LHC: Quartic anomalous couplings, Phys. Rev. D **59**, 015022 (1998).

[31] G. Buchalla and O. Catà, Effective theory of a dynamically broken electroweak standard model at NLO, J. High Energy Phys. 07 (2012) 101.

[32] S. N. Gupta, J. M. Johnson, and W. W. Repko, W, Z and Higgs scattering at SSC energies, Phys. Rev. D **48**, 2083 (1993).

[33] J. Bagger, V. D. Barger, K.-m. Cheung, J. F. Gunion, T. Han, G. A. Ladinsky, R. Rosenfeld, and C. P. Yuan, The strongly interacting WW system: Gold plated modes, Phys. Rev. D **49**, 1246 (1994).

[34] J. Bagger, V. D. Barger, K.-m. Cheung, J. F. Gunion, T. Han, G. A. Ladinsky, R. Rosenfeld, and C.-P. Yuan, CERN LHC analysis of the strongly interacting WW system: Gold plated modes, Phys. Rev. D **52**, 3878 (1995).

[35] V. D. Barger, K.-m. Cheung, T. Han, and R. J. N. Phillips, Probing strongly interacting electroweak dynamics through W^+W^-/ZZ ratios at future e^+e^- colliders, Phys. Rev. D **52**, 3815 (1995).

[36] S. N. Gupta, J. M. Johnson, G. A. Ladinsky, and W. W. Repko, Gauge boson scattering signals at the CERN LHC, Phys. Rev. D **53**, 4897 (1996).

[37] F. Feruglio, The chiral approach to the electroweak interactions, Int. J. Mod. Phys. A **08**, 4937 (1993).

[38] B. Grinstein and M. Trott, A Higgs-Higgs bound state due to new physics at a TeV, Phys. Rev. D **76**, 073002 (2007).

[39] R. Alonso, M. B. Gavela, L. Merlo, S. Rigolin, and J. Yepes, The effective chiral Lagrangian for a light dynamical "Higgs particle," Phys. Lett. B **722**, 330 (2013); **726**, 926 (2013).

[40] R. Alonso, M. B. Gavela, L. Merlo, S. Rigolin, and J. Yepes, Flavor with a light dynamical "Higgs particle," Phys. Rev. D **87**, 055019 (2013).

[41] G. Buchalla, O. Catà, and C. Krause, Complete electroweak chiral Lagrangian with a light Higgs at NLO, Nucl. Phys. **B880**, 552 (2014).

[42] W. Buchmüller and D. Wyler, Effective Lagrangian analysis of new interactions and flavor conservation, Nucl. Phys. **B268**, 621 (1986).

[43] K. Hagiwara, S. Ishihara, R. Szalapski, and D. Zeppenfeld, Low-energy constraints on electroweak three gauge boson couplings, Phys. Lett. B **283**, 353 (1992).

[44] K. Hagiwara, S. Ishihara, R. Szalapski, and D. Zeppenfeld, Low-energy effects of new interactions in the electroweak boson sector, Phys. Rev. D **48**, 2182 (1993).

[45] B. Grzadkowski, M. Iskrzynski, M. Misiak, and J. Rosiek, Dimension-six terms in the Standard Model Lagrangian, J. High Energy Phys. 10 (2010) 085.

[46] J. M. Cornwall, D. N. Levin, and G. Tiktopoulos, Uniqueness of spontaneously broken gauge theories, Phys. Rev. Lett. **30**, 1268 (1973); **31**, 572 (1973).

[47] J. M. Cornwall, D. N. Levin, and G. Tiktopoulos, Derivation of gauge invariance from high-energy unitarity bounds on the S matrix, Phys. Rev. D **10**, 1145 (1974); **11**, 972 (1975).

[48] M. C. Bergere and Y.-M. P. Lam, Equivalence theorem and Faddeev-Popov ghosts, Phys. Rev. D **13**, 3247 (1976).

[49] S. Weinberg, Phenomenological Lagrangians, Physica (Amsterdam) **96A**, 327 (1979).

[50] W. Kilian and K. Riesselmann, The Higgs resonance in vector boson scattering, Phys. Rev. D **58**, 053004 (1998).

[51] Presentations by M. Kado (ATLAS Collaboration) and A. David (CMS Collaboration) at *The 37th Conference on High Energy Physics, Valencia, Spain, 2014*, https://indico.ific.uv.es/indico/contributionDisplay.py?contribId=78&confId=2025, https://indico.ific.uv.es/indico/contributionDisplay.py?contribId=77&confId=2025.

[52] G. Passarino, NLO inspired effective Lagrangians for Higgs physics, Nucl. Phys. **B868**, 416 (2013).

[53] W. Kilian, M. Krämer, and P. M. Zerwas, Anomalous couplings in the Higgsstrahlung process, Phys. Lett. B **381**, 243 (1996).

[54] W. Kilian and J. Reuter, The low-energy structure of little Higgs models, Phys. Rev. D **70**, 015004 (2004).

[55] G. F. Giudice, C. Grojean, A. Pomarol, and R. Rattazzi, The strongly-interacting light Higgs, J. High Energy Phys. 06 (2007) 045.

[56] J. R. Espinosa, C. Grojean, and M. Mühlleitner, Composite Higgs Search at the LHC, J. High Energy Phys. 05 (2010) 065.

[57] E. Boos, V. Bunichev, M. Dubinin, and Y. Kurihara, Higgs boson signal at complete tree level in the SM extension by dimension-six operators, Phys. Rev. D **89**, 035001 (2014).

[58] R. Contino, M. Ghezzi, C. Grojean, M. Mühlleitner, and M. Spira, Effective Lagrangian for a light Higgs-like scalar, J. High Energy Phys. 07 (2013) 035.

[59] K. Hagiwara, R. Szalapski, and D. Zeppenfeld, Anomalous Higgs boson production and decay, Phys. Lett. B **318**, 155 (1993).

[60] S. Alam, S. Dawson, and R. Szalapski, Low-energy constraints on new physics revisited, Phys. Rev. D **57**, 1577 (1998).

[61] C. Grojean, E. E. Jenkins, A. V. Manohar, and M. Trott, Renormalization group scaling of Higgs operators and $\Gamma(h \to \gamma\gamma)$, J. High Energy Phys. 04 (2013) 016.

[62] H. Belusca-Maito, Effective Higgs Lagrangian and constraints on Higgs couplings, arXiv:1404.5343.

[63] A. Biekötter, A. Knochel, M. Krämer, D. Liu, and F. Riva, Vices and virtues of Higgs EFTs at large energy, Phys. Rev. D **91**, 055029 (2015).

[64] J. Elias-Miró, J. R. Espinosa, E. Masso, and A. Pomarol, Renormalization of dimension-six operators relevant for the Higgs decays $h \to \gamma\gamma, \gamma Z$, J. High Energy Phys. 08 (2013) 033.

[65] J. Elias-Miró, J. R. Espinosa, E. Masso, and A. Pomarol, Higgs windows to new physics through $d = 6$ operators: Constraints and one-loop anomalous dimensions, J. High Energy Phys. 11 (2013) 066.

[66] E. E. Jenkins, A. V. Manohar, and M. Trott, Renormalization group evolution of the standard model dimension six operators I: Formalism and lambda dependence, J. High Energy Phys. 10 (2013) 087.

[67] E. E. Jenkins, A. V. Manohar, and M. Trott, Renormalization group evolution of the standard model dimension six operators II: Yukawa dependence, J. High Energy Phys. 01 (2014) 035.

[68] R. Alonso, E. E. Jenkins, A. V. Manohar, and M. Trott, Renormalization group evolution of the standard model dimension six operators III: Gauge coupling dependence and phenomenology, J. High Energy Phys. 04 (2014) 159.

[69] O. J. P. Eboli, M. C. Gonzalez-Garcia, and J. K. Mizukoshi, $pp \to jje^{\pm}\mu^{\mp}\nu\nu$ and $jje^{\pm}\mu^{\mp}\nu\nu$ at $\mathcal{O}(\alpha_{em}^6)$ and $\mathcal{O}(\alpha_{em}^4\alpha_s^2)$ for the study of the quartic electroweak gauge boson vertex at CERN LHC, Phys. Rev. D **74**, 073005 (2006).

[70] C. Degrande, A basis of dimension-eight operators for anomalous neutral triple gauge boson interactions, J. High Energy Phys. 02 (2014) 101.

[71] T. Corbett, O. J. P. Éboli, J. Gonzalez-Fraile, and M. C. Gonzalez-Garcia, Determining Triple Gauge Boson Couplings from Higgs Data, Phys. Rev. Lett. **111**, 011801 (2013).

[72] A. Pomarol and F. Riva, Towards the ultimate SM fit to close in on Higgs physics, J. High Energy Phys. 01 (2014) 151.

[73] P. Sikivie, L. Susskind, M. B. Voloshin, and V. I. Zakharov, Isospin breaking in technicolor models, Nucl. Phys. **B173**, 189 (1980).

[74] G. L. Kane, W. W. Repko, and W. B. Rolnick, The effective W+-, Z0 approximation for high-energy collisions, Phys. Lett. **148B**, 367 (1984).

[75] S. Dawson, The effective W approximation, Nucl. Phys. **B249**, 42 (1985).

[76] W. Kilian, T. Ohl, and J. Reuter, WHIZARD: Simulating multi-particle processes at LHC and ILC, Eur. Phys. J. C **71**, 1742 (2011).

[77] M. Moretti, T. Ohl, and J. Reuter, O'Mega: An optimizing matrix element generator, In *2nd ECFA/DESY Study 1998–2001* 1981–2009, http://inspirehep.net/record/553138?ln=en.

[78] W. Kilian, J. Reuter, S. Schmidt, and D. Wiesler, An analytic initial-state parton shower, J. High Energy Phys. 04 (2012) 013.

[79] C. Degrande, N. Greiner, W. Kilian, O. Mattelaer, H. Mebane, T. Stelzer, S. Willenbrock, and C. Zhang, Effective field theory: A modern approach to anomalous couplings, Ann. Phys. (Amsterdam) **335**, 21 (2013).

[80] W. Heitler, The influence of radiation damping on the scattering of light and mesons by free particles. I., Math. Proc. Cambridge Philos. Soc. **37**, 291 (1941); The

quantum theory of damping as a proposal for Heisenberg's S-matrix, *International Conference on Fundamental Particles and Low Temperatures, 1946, Cambridge, UK*.
[81] J. S. Schwinger, Quantum electrodynamics. I: A covariant formulation, Phys. Rev. **74**, 1439 (1948).
[82] J. Beringer *et al.* (Particle Data Group Collaboration), Review of particle physics (RPP), Phys. Rev. D **86**, 010001 (2012).
[83] F. Bloch and A. Nordsieck, Note on the radiation field of the electron, Phys. Rev. **52**, 54 (1937).
[84] D. R. Yennie, S. C. Frautschi, and H. Suura, The infrared divergence phenomena and high-energy processes, Ann. Phys. (N.Y.) **13**, 379 (1961).
[85] P. P. Kulish and L. D. Faddeev, Asymptotic conditions and infrared divergences in quantum electrodynamics, Teor. Mat. Fiz. **4**, 153 (1970) [Theor. Math. Phys. **4**, 745 (1970)].
[86] H. D. Dahmen, P. Manakos, T. Mannel, and T. Ohl, Unitary approximation for radiative high-energy scattering processes: Application to Bhabha scattering, Z. Phys. C **50**, 75 (1991).
[87] S. N. Gupta, Theory of longitudinal photons in quantum electrodynamics, Proc. Phys. Soc. London Sect. A **63**, 681 (1950).
[88] S. N. Gupta, *Quantum Electrodynamics* (Gordon and Breach, New York, 1981).
[89] M. S. Berger and M. S. Chanowitz, Strong W^+W^+ scattering at the SSC, Phys. Lett. B **263**, 509 (1991).
[90] M. S. Chanowitz, Quantum corrections from nonresonant WW scattering, Phys. Rep. **320**, 139 (1999).
[91] F. Riesz, Über die linearen Transformationen des Hilbertschen Raumes, Acta Sci. Math. (Szeged) **5**, 23 (1930).
[92] I. Gelfand, Normierte Ringe, Recueil Mathématique **9**, 3 (1941).
[93] N. Dunford and J. T. Schwartz, *Linear Operators, Part I: General Theory* (J. Wiley and Sons, New York, 1988); *Linear Operators, Part II: Spectral Theory* (J. Wiley and Sons, New York, 1988).
[94] H. Padé, Sur la répresentation approchée d'une fonction par des fractions rationelles, Thesis, Ann. École Nor. (3), **9**, 193 (1892), supplement.
[95] J. L. Basdevant, D. Bessis, and J. Zinn-Justin, Padé approximants in strong interactions. Two-body pion and kaon systems, Nuovo Cimento A **60**, 185 (1969).
[96] J. L. Basdevant and B. W. Lee, Padé approximation in the sigma model unitary $\pi\pi$ amplitudes with the current algebra constraints, Phys. Lett. **29B**, 437 (1969).
[97] D. A. Dicus and W. W. Repko, Padé approximants and unitarity in W^+W^- and Z^0Z^0 scattering, Phys. Rev. D **42**, 3660 (1990).
[98] A. Dobado, M. J. Herrero, and T. N. Truong, Study of the strongly interacting Higgs sector, Phys. Lett. B **235**, 129 (1990).
[99] A. Dobado, M. J. Herrero, and J. Terron, The role of chiral Lagrangians in strongly interacting $W(l)$ $W(l)$ signals at pp supercolliders, Z. Phys. C **50**, 205 (1991).
[100] A. Dobado, M. J. Herrero, and J. Terron, $W^{\pm}Z^0$ signals from the strongly interacting symmetry breaking sector, Z. Phys. C **50**, 465 (1991).
[101] S. Willenbrock, The Padé and K matrix approximations to the O(2N) model for large N, Phys. Rev. D **43**, 1710 (1991).
[102] T. N. Truong, Chiral Perturbation Theory and Final State Theorem, Phys. Rev. Lett. **61**, 2526 (1988).
[103] T. N. Truong, Remarks on the Unitarization Methods, Phys. Rev. Lett. **67**, 2260 (1991).
[104] A. Dobado and J. R. Pelaez, The inverse amplitude method in chiral perturbation theory, Phys. Rev. D **56**, 3057 (1997).
[105] A. Dobado, M. J. Herrero, J. R. Pelaez, and E. Ruiz Morales, CERN LHC sensitivity to the resonance spectrum of a minimal strongly interacting electroweak symmetry breaking sector, Phys. Rev. D **62**, 055011 (2000).
[106] D. Espriu and F. Mescia, Unitarity and causality constraints in composite Higgs models, Phys. Rev. D **90**, 015035 (2014).
[107] T. N. Truong, Radiative corrections to W(L) W(L) scattering in the standard model, Phys. Lett. B **258**, 402 (1991).
[108] D. Zeppenfeld and S. Willenbrock, Probing the three vector-boson vertex at hadron colliders, Phys. Rev. D **37**, 1775 (1988).
[109] U. Baur and D. Zeppenfeld, Unitarity constraints on the electroweak three vector boson vertices, Phys. Lett. B **201**, 383 (1988).
[110] T. Figy and D. Zeppenfeld, QCD corrections to jet correlations in weak boson fusion, Phys. Lett. B **591**, 297 (2004).
[111] V. Hankele, G. Klämke, D. Zeppenfeld, and T. Figy, Anomalous Higgs boson couplings in vector boson fusion at the CERN LHC, Phys. Rev. D **74**, 095001 (2006).
[112] C. Arzt, M. B. Einhorn, and J. Wudka, Patterns of deviation from the standard model, Nucl. Phys. **B433**, 41 (1995).
[113] V. D. Barger, A. L. Stange, and R. J. N. Phillips, Multiple weak boson signals at hadron supercolliders, Phys. Rev. D **45**, 1484 (1992).
[114] R. J. Eden, P. V. Landshoff, D. I. Olive, and J. C. Polkinghorne, *The Analytic S-Matrix* (Cambridge University Press, Cambridge, UK, 1966).
[115] E. N. Argyres, W. Beenakker, G. J. van Oldenborgh, A. Denner, S. Dittmaier, J. Hoogland, R. Kleiss, C. G. Papadopoulos, and G. Passarino, Stable calculations for unstable particles: Restoring gauge invariance, Phys. Lett. B **358**, 339 (1995).
[116] N. D. Christensen, C. Duhr, B. Fuks, J. Reuter, and C. Speckner, Introducing an interface between WHIZARD and FeynRules, Eur. Phys. J. C **72**, 1990 (2012).
[117] W. Kilian, J. Reuter, and M. Sekulla (to be published).